

2016

# Construction of an optical fiber strain gauge

Najwa Sulaiman

Follow this and additional works at: <https://commons.emich.edu/theses>

Part of the [Astrophysics and Astronomy Commons](#), and the [Physics Commons](#)

---

## Recommended Citation

Sulaiman, Najwa, "Construction of an optical fiber strain gauge" (2016). *Master's Theses and Doctoral Dissertations*. 869.  
<https://commons.emich.edu/theses/869>

This Open Access Thesis is brought to you for free and open access by the Master's Theses, and Doctoral Dissertations, and Graduate Capstone Projects at DigitalCommons@EMU. It has been accepted for inclusion in Master's Theses and Doctoral Dissertations by an authorized administrator of DigitalCommons@EMU. For more information, please contact [lib-ir@emich.edu](mailto:lib-ir@emich.edu).

Construction of an Optical Fiber Strain Gauge

by

Najwa Sulaiman

Thesis

Submitted to the Department of Physics and Astronomy

Eastern Michigan University

in partial fulfillment of the requirements

for the degree of

MASTER OF SCIENCE

in

Physics

Thesis Committee:

Ernest Behringer, Ph.D, Chair

Marshall Thomsen, Ph.D.

Eric Paradis, Ph.D.

April 8, 2016

Ypsilanti, Michigan

## **Dedication**

To my beloved country

**Iraq**

To My Grandparents

**Fatima, Zainab, Sulaiman and Ali Asghar**

To My parents

**Ameena and Ibrahim**

## Acknowledgments

First and foremost, I thank **Allah (God)**, praised and exalted is He, for giving me patience and helping me finish this thesis.

I owe my gratitude to all those people who have supported, encouraged, and helped me to accomplish this thesis.

I thank the **government of Iraq** and **The Higher Committee for Education Development in Iraq** for the financial support and having faith in me.

My deepest gratitude and my respect to my advisor, **Dr. Ernest Behringer**, for his valuable advices and guidance. I am grateful to him for supporting and helping me to overcome many crisis situations and finish this thesis.

Also, I thank **Dr. Marshall Thomsen** and **Dr. Eric Paradis** for their insightful comments and help.

I thank the **Department of Physics and Astronomy** for support of this research.

My great appreciation to my parents who have always been there through thick and thin, whenever I needed them. Their prayers gave me the strength to go on.

Special thanks to my sisters and brothers for their help, especially my brother **Nabeel Sulaiman**, who supports my ambitions and helps me to fulfill my dreams.

Also, many thanks to my grandfather who encourages me constantly. In addition, I thank my aunts and uncles for their encouragement.

My sincerest thanks to my guarantors for their trust and help.

Last but not the least, I thank all my friends for their true friendship, in particular **Saja Albuarabi**, who was with me throughout the most difficult times as well as good moments.

## **Abstract**

This project is focused on the construction of an optical fiber strain gauge that is based on a strain gauge described by Butter and Hocker. Our gauge is designed to generate an interference pattern from the signals carried on two bare single-mode fibers that are fastened to an aluminum cantilever. When the cantilever experiences flexural stress, the interference pattern should change. By observing this change, it is possible to determine the strain experienced by the cantilever. I describe the design and construction of our optical fiber strain gauge as well as the characterization of different parts of the apparatus.

## Table of Contents

Dedication.....	ii
Acknowledgments.....	iii
Abstract.....	iv
Chapter One: Introduction and Literature Review.....	1
1. Introduction.....	1
2. Literature Review.....	3
Chapter Two: Reference Work and Theoretical Basis .....	10
Chapter Three: Methodology and The Optical Alignment.....	19
1. Methodology.....	19
2. The Optical Alignment .....	20
Chapter Four: Data and Analysis.....	23
1. Sensitivity of Optical Fiber Strain Gauge.....	23
2. Measuring the Beam Profile .....	25
A. Determination of the Beam Profile Using the Knife-Edge Method: Experimental Method, Data, and Analysis .....	25
B. Determination of the Beam Profile Using an Optical Fiber: Experimental Method, Data, and Analysis .....	30
3. Measuring the Efficiency of Coupling the Free Space Beam to the Fiber: Experimental Method, Data, and Analysis .....	34
Chapter Five: Summary .....	39
References.....	40
APPENDIX A: PYTHON CODES .....	43

a. PYTHON CODE FOR CALCULATING THE STRAIN GAUGE SENSITIVITY.....	43
b. PYTHON CODE FOR PLOTTING THE RAW POWER AND STAGE READINGS FOR THE BEAM PROFILE—KNIFE-EDGE METHOD .....	45
c. PYTHON CODE FOR PLOTTING THE CORRECTED POWER AND STAGE READINGS FOR THE BEAM PROFILE—KNIFE-EDGE METHOD .....	46
d. PYTHON CODE FOR EVALUATING THE LASER BEAM DIAMETER FOR BEAM PROFILE—KNIFE-EDGE METHOD .....	48
e. PYTHON CODE FOR PLOTTING THE RAW POWER AND STAGE READINGS FOR THE BEAM PROFILE—SINGLE-MODE OPTICAL FIBER.....	50
f. PYTHON CODE FOR EVALUATING THE LASER BEAM DIAMETER FOR BEAM PROFILE—SINGLE-MODE OPTICAL FIBER.....	52
g. PYTHON CODE FOR PLOTTING THE SENSITIVITY OF THE COUPLING OF THE FREE SPACE BEAM TO THE FIBER .....	55
APPENDIX B: CALCULATIONS FOR BEAM PROFILE.....	57
a. CALCULATING THE DIAMETER OF A BEAM.....	57
b. CALCULATING $I_{0mn}$ .....	58

## List of Figures

Fig. 1: A diagram to illustrate the definition of strain .....	2
Fig. 2: Reproduction of Fig. 1 from Ref. 7. (a) Point sensor. (b) Intrinsic distributed sensor. (c) Quasi-distributed sensor.....	3
Fig. 3: Reproduction of Fig. 1 from Ref. 8. A schematic diagram showing the periodic phase gratings.....	5
Fig. 4: The apparatus described by Pomarico, Sicre, Patrignani, and De Pasquale.....	6
Fig. 5: Reproduction of Fig. 1 from Ref. 10. Tapered single-mode optical fiber.....	7
Fig. 6: The apparatus described by Arregui <i>et al.</i> to study optical fiber strain gauge with a resistive gauge.....	8
Fig. 7: Reproduction of Fig. 2 from Ref. 11. The extrinsic Fabry-Perot interferometer .....	9
Fig. 8: Reproduction of Fig. 1 of Ref. 5. Apparatus for measuring optical fiber strain described by Butter and Hocker.....	10
Fig. 9: The shear force diagram and bending moment diagram for a cantilever loaded at its free end at $x = l$ .....	11
Fig. 10: The cantilever before and after it is loaded .....	12
Fig. 11: A schematic diagram of the optical fiber strain gauge .....	19
Fig. 12: Setup for optical pre-alignment.....	21
Fig. 13: Setup for the optical fiber strain measurement.....	22
Fig. 14: A contour plot of the sensitivity versus strain-optic tensor elements for a fiber mode diameter of $5.3 \mu\text{m}$ .....	24
Fig. 15: A contour plot of the sensitivity versus strain-optic tensor elements for a fiber mode diameter of $3.6 \mu\text{m}$ .....	25



Fig. 16: A schematic diagram of the apparatus for using the knife-edge technique for determining the beam profile .....	26
Fig. 17: A photograph of the experimental setup for using the knife-edge technique to determine the beam profile .....	26
Fig. 18: Plot of the raw power reading versus the raw stage reading .....	27
Fig. 19: Plot of $\frac{P(x)-P_{bkgd}}{P_{max}}$ versus $x_{1/2} - x$ .....	28
Fig. 20: Plot of $\frac{P(x)-P_{bkgd}}{P_{max}}$ versus $x_{1/2} - x$ with the fit function .....	29
Fig. 21: A schematic diagram of the apparatus for using the single-mode optical fiber to determine the beam profile .....	30
Fig. 22: The apparatus for using the single-mode optical fiber cable for determining the beam profile .....	31
Fig. 23: Plot of the raw stage reading versus the transmitted power .....	32
Fig. 24: Comparison of the beam profile measured with the optical fiber to the theoretical beam profile when $w = 250 \mu m$ .....	33
Fig. 25: Comparison of the beam profile measured with the optical fiber to the theoretical beam profile when $w = 260 \mu m$ .....	33
Fig. 26: Comparison of the beam profile measured with the optical fiber to the theoretical beam profile when $w = 270 \mu m$ .....	34
Fig. 27: A schematic diagram of the apparatus for measuring the sensitivity of the coupling of the free space beam to the fiber .....	35
Fig. 28: The apparatus for measuring the sensitivity of the coupling of the free space beam to the fiber .....	36
Fig. 29: Fiber coupling sensitivity .....	37

## Chapter One: Introduction and Literature Review

### 1. Introduction

During the last fifty years, the optical fiber has been developed and exploited in a variety of applications such as telecommunication systems, power transmission, and sensors. Optical fiber sensors are used for measuring quantities such as strain, temperature, and the load reliability of civil structures.<sup>1</sup> This shows the importance of optical fiber sensors. Because of its important applications, the demand for highly sensitive sensors, especially strain sensors, is increasing. For this reason, we chose to build an optical fiber-based strain gauge. Optical fiber-based strain gauges were developed after electrical resistance-based gauges, which use a metallic wire as the strain transducer instead of an optical fiber.<sup>2</sup> The resistance of such a wire depends on both strain and temperature.<sup>2</sup> These wires are made of different alloys, such as nickel-chromium alloys, platinum alloys, and copper-nickel alloys. The electrical resistance-based strain gauges can be inexpensive: for example, one 3-element rosette (Omega SGD-1/120-RY21) costs approximately \$28.<sup>3</sup> However, they are not as accurate as the optical fiber strain gauges. The resistance-based strain gauges have uncertainties ranging from  $(\pm 2.1 \mu\epsilon$  to  $\pm 50.08 \mu\epsilon)$ .<sup>4</sup> Consequently, the aim of this project is to measure the strain of a cantilever by using an optical fiber strain gauge. After completing these measurements, we should be able to answer the following questions: Can we build an optical based strain gauge? If so, what is its sensitivity?

This thesis is organized as follows. The current chapter provides an introduction to the concepts of stress and strain and a brief review of the literature. The second chapter provides more details about the optical strain gauge described by Butter and Hocker.<sup>5</sup> The third chapter provides a description of the apparatus and experimental methods. The fourth chapter presents the data and an analysis of the data. Finally, the fifth chapter is a summary of this project.

Stress is defined as the force per unit of a cross sectional area. Applied stress causes a material to deform. The average value of stress can be calculated as  $\sigma = \frac{F}{A}$ , where  $\sigma$  is the average stress,  $F$  is the force applied to the cross section, and  $A$  is the area of the cross section. The strain can be defined as the scaled deformation of a body resulting from an applied stress. We illustrate these concepts in Fig.1, which shows a bar that experiences axial forces.

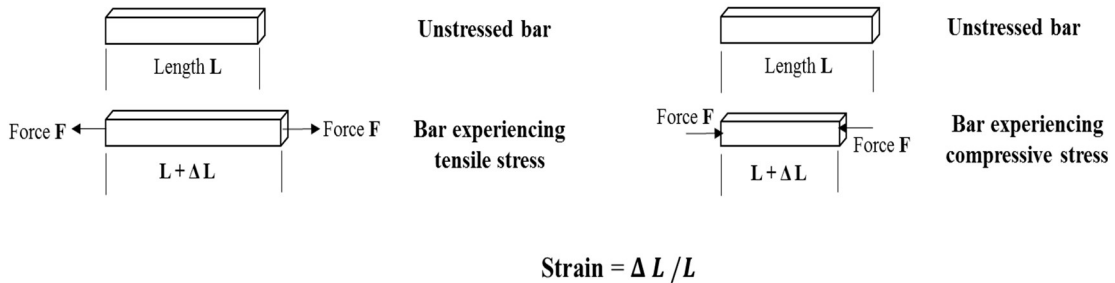


Fig. 1: A diagram to illustrate the definition of strain.

Figure 1 illustrates how a bar undergoes a change in length  $\Delta L = L_f - L$  after experiencing tensile or compressive forces. The strain is the ratio  $\Delta L/L$ , where  $L$  is the original length of the bar and  $\Delta L$  is the difference between the final length and the original length of the bar. The strain is unitless. The change in length can be positive in the case of tensile forces or negative in case of compressive forces.<sup>6</sup> The symbol for the strain that will be used in this project is  $\epsilon$ .<sup>6</sup>

The strain in an optical fiber is the scaled change of its optical path-length due to an applied stress. This change is caused by changes in the refractive indices of the core and cladding of the optical fiber as well as by changes in the physical dimensions of the fiber. Consequently, the optical fiber strain can be determined by observing the interference pattern produced when light transmitted by the fiber overlaps with the light transmitted through a reference fiber.

## 2. Literature Review:

There are different types of optical fiber sensors for measuring strain that can be classified into three categories according to spatial resolution: point sensor,<sup>7</sup> intrinsic distributed sensors, and quasi-distributed sensors.<sup>7</sup> Point sensors are used for measuring a specific measurand at a specific point.<sup>7</sup> Intrinsic distributed sensors can measure the measurand along the optical fiber.<sup>7</sup> Quasi-distributed sensors are sensors that measure the measurand at more than one point along the length of the optical fiber.<sup>7</sup> Fig. 2 shows the three types of the sensors.

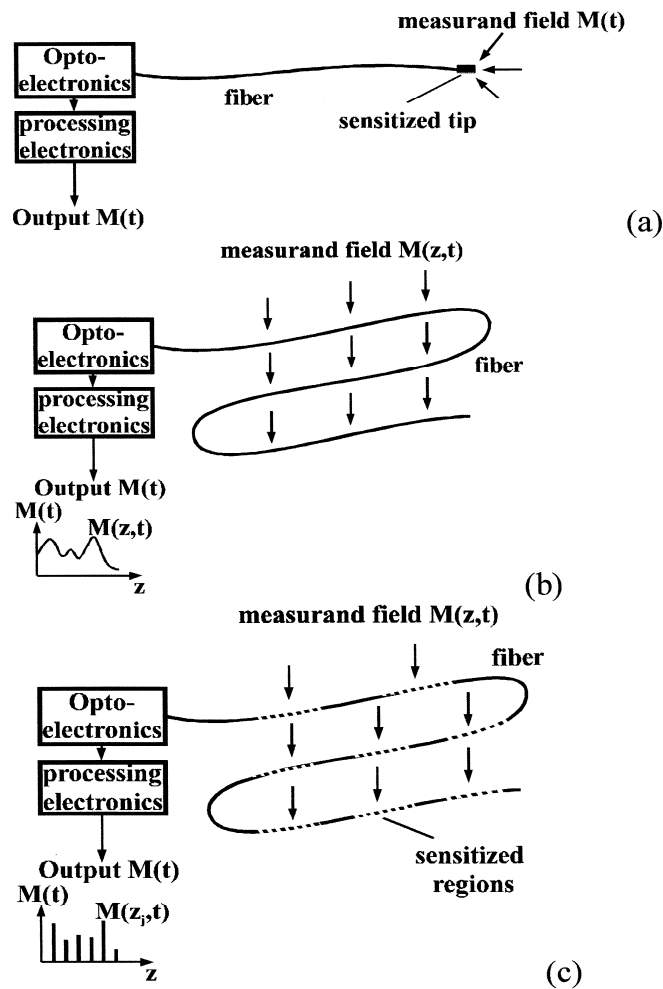


Fig. 2: Reproduction of Fig. 1 from Ref. 7. (a) Point sensor. (b) Intrinsic distributed sensor. (c) Quasi-distributed sensor.

The different types of optical fiber sensors can also be classified into categories according to the main concept that each one uses: interferometric sensors, distributed fiber optic sensors, luminescent optical fiber sensors, plastic optical fiber sensors, and in-fiber Bragg grating sensors.<sup>7</sup> Interferometric optical fiber sensors are based on the concept of superposing two signals.<sup>7</sup> Distributed fiber optic sensors exploit the concept of light scattering.<sup>7</sup> Luminescent optical fiber sensors are based on causing the fiber to luminesce by doping it with materials such as neodymium and erbium.<sup>7</sup> Plastic optical fiber sensors are based on using optical fibers that are made of plastic, which have the advantage of low cost and the disadvantage of data loss.<sup>7</sup> In-fiber Bragg grating sensors are based on the idea of writing Bragg gratings, which are simple elements for sensing, into optical fiber cables.<sup>7</sup> One of the probable applications of in-fiber Bragg grating sensors' is monitoring strain.<sup>7</sup> This is accomplished by determining the shift in the Bragg condition compared to an optical path.<sup>7</sup> The optical fiber cable is used in this method to obtain higher sensitivity.<sup>7</sup> Although this sensor can be a good strain monitor, interferometric sensing is more useful.<sup>7</sup>

Having described the different categories of optical strain sensors, we proceed to discuss some of the early work that has been done in measuring strain using optical fiber. C.D. Butter and G.B. Hocker determined the strain experienced by the surface of a cantilever by using an optical fiber strain gauge constructed from two bare single-mode optical fibers glued on the cantilever.<sup>5</sup> Their purpose for building this gauge was to create a sensitive optical fiber strain gauge to measure the strain in any structure to which these fibers are attached.<sup>5</sup> Because our project is a modified version of this gauge, more information will be given in chapter two.

Meltz, Glenn, and Snitzer followed a different approach to measure the optical fiber strain. They used periodic phase gratings in the core of an optical fiber,<sup>8</sup> as shown in Fig. 3.

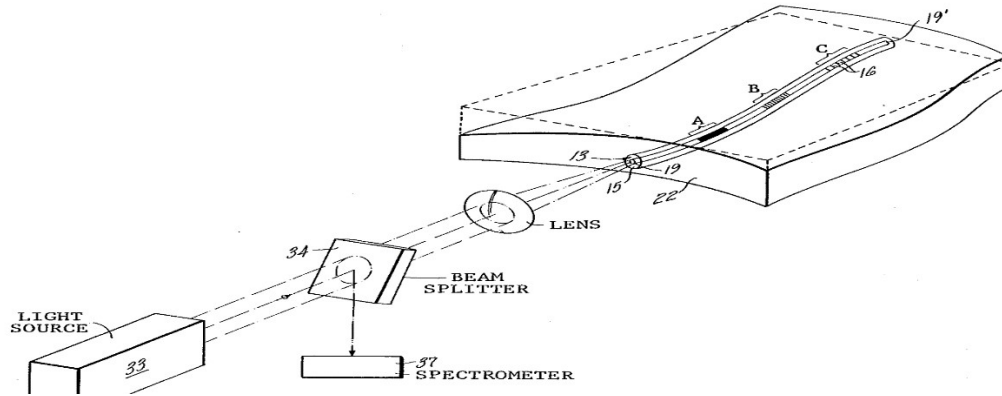


Fig 3: Reproduction of Fig. 1 from Ref. 8. A schematic diagram showing the periodic phase gratings.

As the figure shows, a laser light source sends the light into a beam splitter which divides the light into two beams.<sup>8</sup> One beam is directed towards a spectrometer, which measures the amount of absorbed light.<sup>8</sup> The other beam is directed towards a lens, which focuses the light into the core of an optical fiber.<sup>8</sup> A, B, and C are the regions of the fiber core where the wavelength gratings were written.<sup>8</sup> The wavelength gratings were generated by transversely directed ultraviolet radiation.<sup>8</sup> The gratings were designed to work with different chosen angles of incidence.<sup>8</sup> The fiber core was made of either glass or Germanium-doped silica.<sup>8</sup> The core was attached to a specific plate or part of construction.<sup>8</sup> Depending on the strain experienced by the gratings, the grating period will change, leading to different Bragg conditions and shifts in the peaks in the reflected intensity. The magnitude of the shifts are a measure of the strain.

Pomarico, Sicre, Patrignani, and De Pasquale suggested using an intrinsic optical fiber sensor to measure the strain of surfaces.<sup>9</sup> For this purpose, they used two multimode optical fibers following the interferometric sensors method.<sup>9</sup> They used a HeNe Laser as a light source.<sup>9</sup> The light was divided by a beam splitter into two beams that were focused into two separate multimode fibers.<sup>9</sup> One of the multimode fibers was set up as a reference fiber.<sup>9</sup> The other fiber was set up as the strained fiber which was fastened to translation stages by epoxy.<sup>9</sup> Both fibers

direct the transmitted light through them into a CCD camera sensor.<sup>9</sup> The distance that separated the ends of the fibers, which was adjustable for selecting the speckle size, was denoted by  $d$ . The camera was connected to image processing unit to record the images.<sup>9</sup> Fig. 4 illustrates the apparatus.

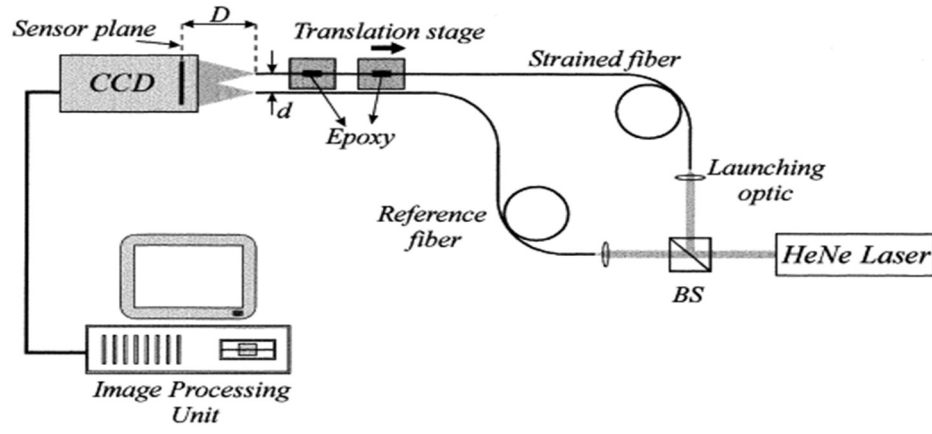


Fig. 4: The apparatus described by Pomarico, Sicre, Patrignani, and De Pasquale.

Pomarico, Sicre, Patrignani, and De Pasquale selected the multimode fiber for this project because of its wide core compared to the single-mode fiber.<sup>9</sup> Their aim was to allow as many modes of light as possible, which, because of their different optical paths, will form an interference pattern.<sup>9</sup> These patterns will generate a specific intensity distribution that is comparable to a speckle pattern.<sup>9</sup> This intensity distribution will be modified when the fiber is strained because of the changes in the phase of the light wave.<sup>9</sup> The intensity pattern of the strained fiber is compared to that of the reference fiber by spatial correlation.<sup>9</sup> After performing a specific calibration that depends on  $d$ , Pomarico *et al.* claimed that their results showed the ability to measure sub-micrometer deformations.<sup>9</sup>

Arregui, Matias, and Lopez-Amo followed a different approach to build an optical fiber strain gauge with low cost.<sup>10</sup> They achieved that by building a tapered single-mode optical

fiber.<sup>10</sup> They built the tapered fiber by dividing the fiber into three regions—contracting, waist, and expanding tapered regions—as illustrated in Fig. 5.<sup>10</sup>

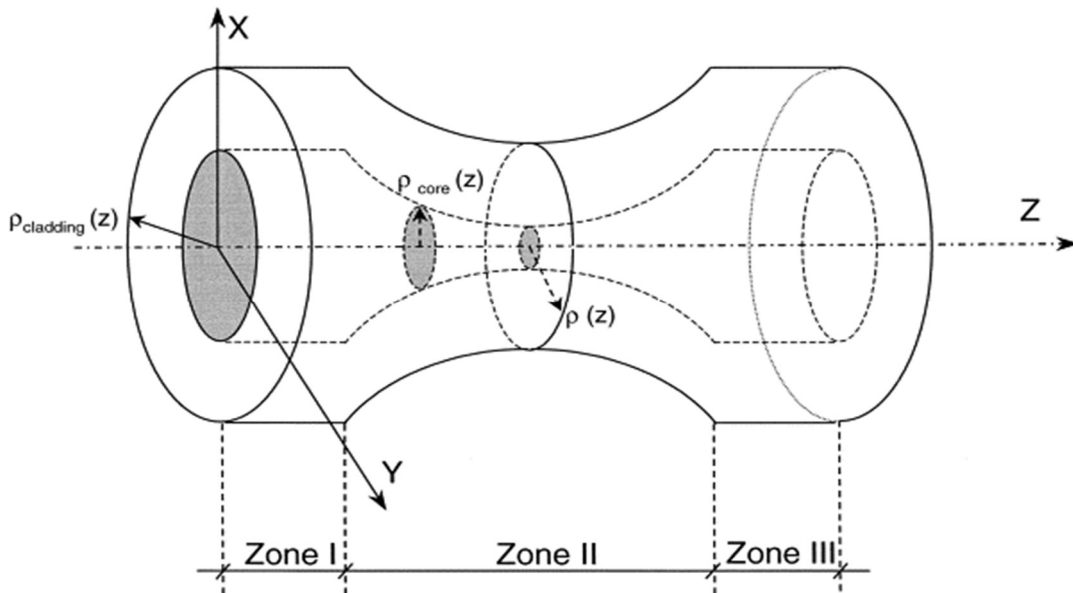


Fig. 5: Reproduction of Fig. 1 from Ref. 10. Tapered single-mode optical fiber.

As shown in Fig. 5, zone I is the contracting part of the fiber where the fiber profile is contracting, zone II is the waist, and zone III is the expanding area.<sup>10</sup> First, they generated the tapered fiber from graded index single-mode fiber.<sup>10</sup> They used an organic solvent to remove the cover of 10 cm sample of the original 2 m of single-mode fiber.<sup>10</sup> They then tapered the uncoated area of the fiber. The process of tapering was accomplished by stripping portions of the fiber and then stretching the stripped portions.<sup>10</sup> After that, “they fixed it onto two symmetrical points with respect to the tapered zone on a micrometer using adhesive cyanocrilate.”<sup>10</sup> By fixing the tapered fiber on the two points, they characterized the optical fiber strain gauge.<sup>10</sup> They found that the optimum of the optical fiber strain gauge can be obtained by selecting the tapered fiber’s waist diameter.<sup>10</sup> Then, they measured the strain of an aluminum cantilever using the two best optical fiber strain gauges according to their characterization. The setup that they built is illustrated in Fig. 6.



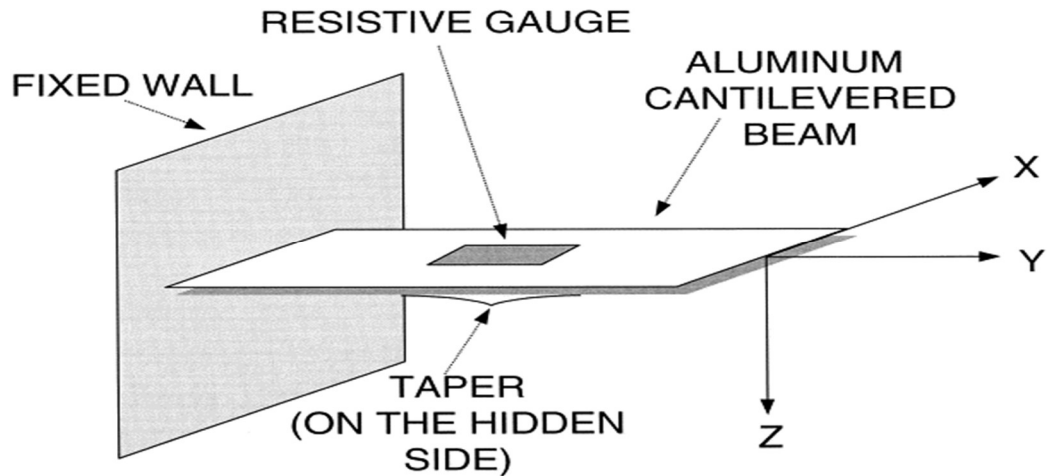


Fig. 6: The apparatus described by Arregui *et al.* to study optical fiber strain gauge with a resistive gauge.

As Fig. 6 shows, the tapered fiber is fixed on the cantilever. They found that the 52  $\mu\text{m}$  optical fiber strain gauge has a measurement range bigger than that of both resistive gauges and Bragg grating gauges.<sup>10</sup> They claim that these results show that gauge designing can be done by choosing certain tapers for different applications of gauges.<sup>10</sup>

Unlike Pomarico *et al.*, Jiang and Gerard developed an extrinsic optical fiber strain gauge.<sup>11</sup> For this purpose, they replaced the cavity of a Fabry-Perot interferometer with a thin transparent film that services as a low finesse Fabry-Perot interferometer.<sup>11</sup> Also, instead of the two mirrors of different reflectivity of the original Fabry-Perot interferometer, they used the ends of two optical fibers as mirrors<sup>11</sup> as shown in Fig. 7.

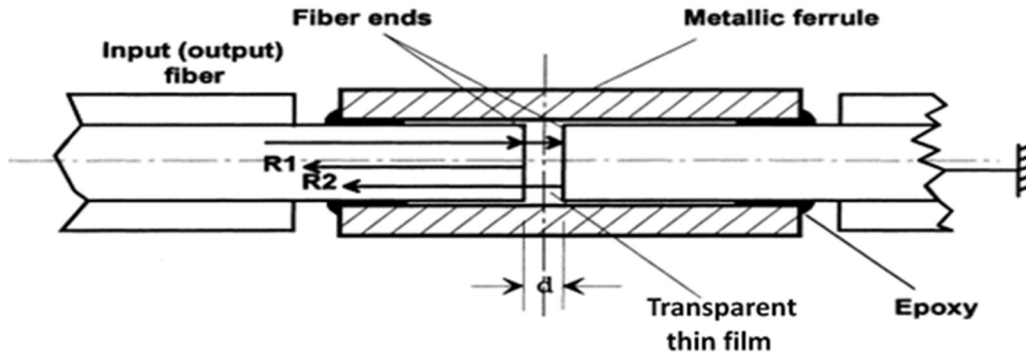


Fig. 7: Reproduction of Fig. 2 from Ref. 11. The extrinsic Fabry-Perot interferometer.

Fig. 7 shows the extrinsic Fabry-Perot interferometer made by gluing two optical fibers to a metal connector while the two ends of the fiber are separated by a thin film. Jiang and Gerard used a thin film that is made of polyurethane.<sup>11</sup> They claim that the transparent thin film reduces the defects of the original setup.<sup>11</sup> Also, the film material gave them the advantage of having two-phases of the film, soft and hard segments which added properties to the setup.<sup>11</sup> Jiang and Gerard stated that the accuracy of the gauge reached  $5 \times 10^{-6}$ .<sup>11</sup> Moreover, they stated that this gauge can be used as a gauge of other parameters such as pressure.<sup>11</sup>

## Chapter Two: Reference Work and Theoretical Basis

As stated in the abstract, this project is an attempt to build an optical fiber strain gauge that is based on the gauge described by Butter and Hocker.<sup>5</sup> Their apparatus is shown in Fig. 8.

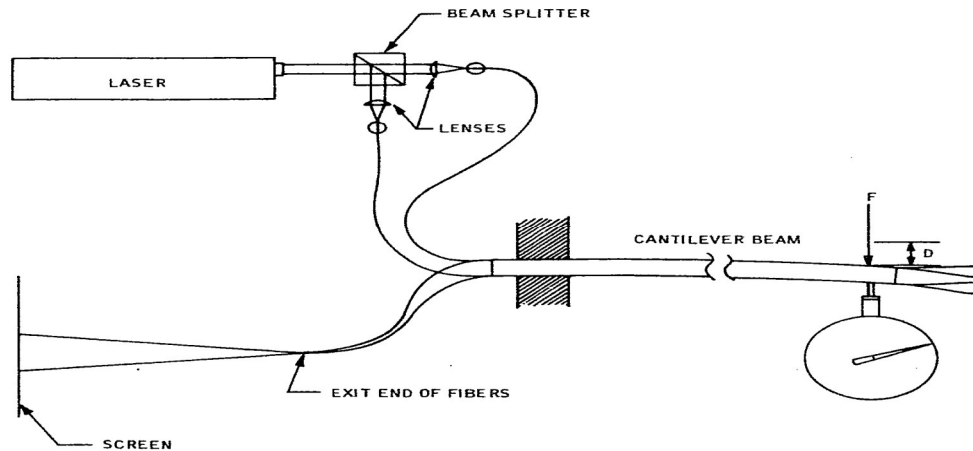


Fig. 8: Reproduction of Fig. 1 of Ref. 5. Apparatus for measuring optical fiber strain described by Butter and Hocker.

As Fig. 8 shows, the laser light is divided by a beam splitter to pass through the two bare single-mode fibers. This laser is supposed to have a coherence length much longer than the optical path length difference between the two paths. A transverse force  $F$  is applied to the cantilever, which causes the cantilever to bend, thereby stretching or compressing the two bare fibers attached to it. Butter and Hocker determined the strain by observing the shift in the interference pattern that was generated by the overlap of the light from both optical fiber cables. This shift was a result of the change in the optical path-length in the fibers.<sup>5</sup> By observing the change in the interference pattern, they claimed that the optical fiber strain gauge is able to measure strains of  $< 0.4 \times 10^{-6}$ . Our project is a modified version of this experiment, with the aim of simplifying the setup and specifying experimental details needed to obtain reproducible results.

The theoretical basis of this experiment was described by C.D. Butter and G.B. Hocker.<sup>5</sup> A more detailed version of that description, based on notes by Dr. E. Behringer, is presented below.

First, we will describe how to obtain an expression for the strain in the fibers using concepts from engineering mechanics. We begin by presenting the shear force and bending moment diagrams for a cantilever that is subject to a concentrated load  $P$  at its free end.

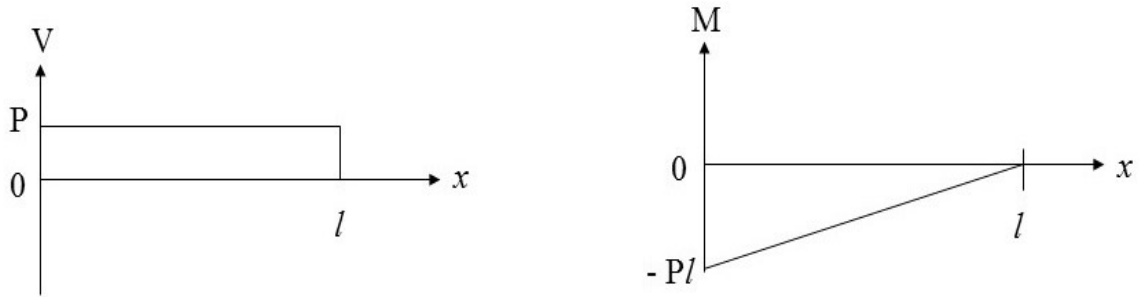


Fig. 9: The shear force diagram and bending moment diagram for a cantilever loaded at its free end at  $x = l$

From the shear force diagram, we see that the shear force  $V$  is

$$V(x) = P \quad 0 \leq x \leq l \quad (1)$$

where  $l$  is the cantilever length. Then the bending moment,  $M$ , is obtained by considering the shear force diagram in Fig. 9 and applying the relation  $V = \frac{dM}{dx}$ :

$$M(x) = -P(l - x) \quad 0 \leq x \leq l \quad (2)$$

we note that  $M(x = 0) = -Pl$  and  $M(x = l) = 0$  as expected at the fixed end ( $x = 0$ ) and the free end ( $x = l$ ). By the flexure formula, the flexural stress is

$$\sigma = \frac{-My}{I} = -\left(\frac{-P(l - x)y}{I}\right) \quad (3)$$

where  $\sigma$  is the axial stress,  $M$  is the moment in the  $y$  direction,  $y$  is the vertical position in the cross section relative to the neutral plane, and  $I$  is the moment of inertia. Note that the load  $P$  is positive and  $y$  is positive for locations in the cross section between the neutral surface and the surface to which the load is applied. If we let the cantilever have width  $b$  and height  $h = 2a$ , then its moment of inertia is

$$I = \frac{1}{12} bh^3 = \frac{1}{12} b(2a)^3 = \frac{2}{3} ba^3 = \frac{1}{3} b(2a)a^2 = \frac{1}{3} Aa^2 \quad (4)$$

where  $A = b(2a)$  is the cross sectional area of the cantilever. Substitution of (4) into (3) gives

$$\sigma = \frac{3P}{A} \frac{(l-x)a}{a^2} \Rightarrow \sigma = \frac{3P}{A} \frac{(l-x)}{a} \quad (5)$$

where we set  $y = +a$  because  $y$  is the vertical height from the neutral axis of the cantilever and hence  $y = \frac{h}{2}$ . The positive sign for  $a$  is to refer to the distance between the neutral surface and the surface to which the load is applied. The result for  $\sigma$  will be positive, which indicates tensile stress. When the load acts on the free end of the cantilever, the cantilever bends and the free end is displaced by  $d$ . Fig. 10 illustrates the displacement of the cantilever after the cantilever is loaded.

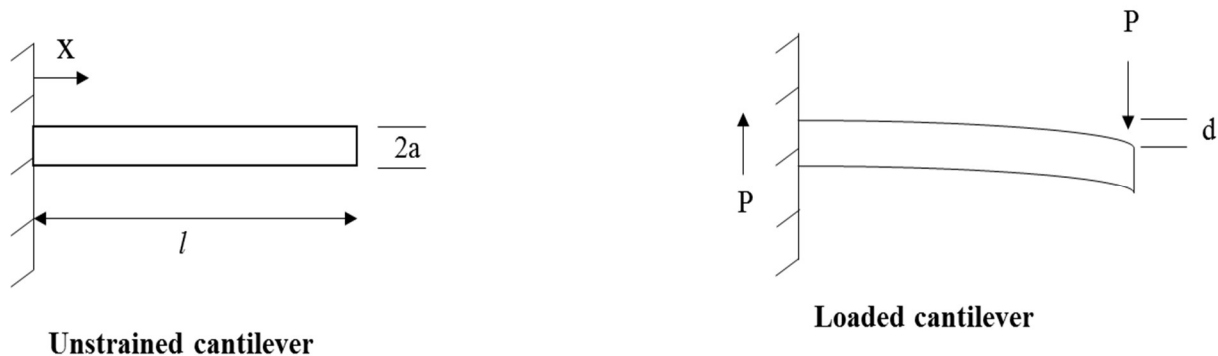


Fig. 10: The cantilever before and after it is loaded.

The displacement of the end of the cantilever  $d$ , shown in Fig. 10, is obtained from the textbook by Gere and Goodno<sup>6</sup>:

$$d = \frac{-Pl^3}{3EI} = \frac{-Pl^3}{EAa^2} \quad (6)$$

where we substituted (4) for  $I$ , and  $E$  is the elastic modulus. This displacement is related to the stress by dividing (5) by  $E$  and then substituting for  $P/EA$  using (6):

$$\epsilon = \frac{\sigma}{E} = \frac{3P(l-x)}{EA} \frac{1}{a} = -3 \frac{da^2(l-x)}{l^3} \frac{1}{a} = \frac{-3da(l-x)}{l^3} \quad (7)$$

This is similar to Eq. (9) of Butter and Hocker, which has  $x$  in place of  $(l-x)$  here. We would get their result if we assumed  $M(x) = -Px$  but this cannot be correct if  $x = 0$  is at the fixed end. If they have chosen  $x = 0$  at the free end, then their Eq. (9) is correct, but the fixed end would be at  $x = -l$ . Therefore, to relate  $x$  here to the position  $x_{BH}$  used by Butter and Hocker, we use

$$x_{BH} = x - l \Rightarrow x = x_{BH} + l \quad (8)$$

Then,

$$l - x = l - (x_{BH} + l) = -x_{BH} \quad (9)$$

so their Eq. (9) is

$$\epsilon = \frac{3da x_{BH}}{l^3} = \frac{3da [-(l-x)]}{l^3} = \frac{-3da(l-x)}{l^3} \quad (10)$$

which agrees with (7). The average strain over the length of the fiber is

$$\bar{\epsilon} = \frac{1}{l} \int_0^l \epsilon(x) dx = \frac{1}{l} \int_0^l \frac{-3da(l-x)}{l^3} dx = \frac{1}{l} \frac{3da}{l^3} \int_0^l (x-l) dx \quad (11)$$

Let  $u = x - l \Rightarrow du = dx$

$$\bar{\epsilon} = \frac{1}{l} \frac{3da}{l^3} \int_{-l}^0 u du = \frac{1}{l} \frac{3da}{l^3} \frac{1}{2} u^2 \Big|_{-l}^0 = \frac{1}{l} \frac{3da}{l^3} \left( \frac{-l^2}{2} \right) \quad (12)$$

$$\bar{\epsilon} = \frac{-3da}{2l^2} \quad (13)$$

Because the displacement of the free end  $d < 0$ , this is a positive (tensile) strain. This result agrees with Eq. (10) of Butter and Hocker. The numbers that Butter and Hocker used to calculate  $\bar{\epsilon}$  are  $l = 0.30 \text{ m}$ ,  $d = 10.28 \times 10^{-6} \text{ m}$  for one fringe shift, and  $a = 0.25 \times 10^{-2} \text{ m}$ .

The average strain is

$$\bar{\epsilon} = \frac{-3(-10.28 \times 10^{-6} \text{ m})(0.25 \times 10^{-2} \text{ m})}{2(0.30 \text{ m})^2} = 4.28 \times 10^{-7} \quad (14)$$

We cannot explain why Butter and Hocker reported that  $\bar{\epsilon} = 4.35 \times 10^{-7}$ .

We now discuss the optics-related part of the calculations with the goal of relating optical properties of the fiber to the average strain in the fiber. The light wave traveling through a fiber of length  $L$  accumulates a phase  $\phi$  defined as

$$\phi = \beta L \quad (15)$$

where  $\beta$  is the propagation constant for that mode (we have a single-mode fiber). If we strain the fiber, its propagation constant and the length will change, so the change in phase is

$$\Delta\phi = \beta\Delta L + L\Delta\beta \quad (16)$$

Because  $\Delta L = \epsilon L$ , this becomes

$$\Delta\phi = \beta\epsilon L + L\Delta\beta \quad (17)$$

The change  $\Delta\beta$  arises from two effects, as noted by Butter and Hocker: first, there is the strain-optics effect, where strain changes the refractive index; and second, there is a waveguide mode dispersion effect, where the change in the core diameter  $D$  changes the mode.

The second term of (17) is then

$$L\Delta\beta = L \frac{d\beta}{dn} \Delta n + L \frac{d\beta}{dD} \Delta D \quad (18)$$

The propagation constant  $\beta$  may be expressed as

$$\beta = n_{eff}k_o \quad (19)$$

where  $n_{core} < n_{eff} < n_{clad}$  and  $k_o = \frac{2\pi}{\lambda_o}$ . Because  $\frac{n_{core}-n_{clad}}{n_{core}} \approx 0.01$ , it is a reasonable approximation to write

$$\beta \approx nk_o \quad (20)$$

Then,

$$\frac{d\beta}{dn} = k_o = \frac{\beta}{n} \quad (21)$$

The change in refractive index  $\Delta n$  is obtained from the relation

$$\Delta\left(\frac{1}{n^2}\right)_i = \sum_{j=1}^6 P_{ij} S_j \quad (22)$$

which is the change in the optical indicatrix.  $S_j$  is the strain vector, and  $P_{ij}$  is the strain-optic tensor.

The strain vector for the situation here is

$$S_j = \begin{bmatrix} \epsilon \\ -\mu\epsilon \\ -\mu\epsilon \\ 0 \\ 0 \\ 0 \end{bmatrix} \quad (23)$$

where  $\mu$  is the Poisson's ratio for the fiber material.

For a homogeneous isotropic medium,  $P_{ij}$  has only two non-zero numerical values,  $P_{11}$  and  $P_{12}$ .

The change in the optical indicatrix in the y and z directions is then

$$\Delta\left(\frac{1}{n^2}\right)_{2,3} = \epsilon(1 - \mu)P_{12} - \mu\epsilon P_{11} \quad (24)$$

Butter and Hocker claim that

$$\Delta n = \frac{-1}{2} n^3 \Delta\left(\frac{1}{n^2}\right)_{2,3} \quad (25)$$



which comes from  $\Delta\left(\frac{1}{n^2}\right) = \frac{-2}{n^3}\Delta n$ . Substitution of (24) into (25) gives

$$\Delta n = \frac{-1}{2}n^3[\epsilon(1-\mu)P_{12} - \mu\epsilon P_{11}] \quad (26)$$

Equations (26) and (21) can be used in (18) to evaluate the first term on the right side of (18).

We turn to the second term on the right side of (18). The change in the diameter of the fiber is

$$\Delta D = -\mu\epsilon D \quad (27)$$

Note that Butter and Hocker neglect the minus sign in (27);  $\Delta D < 0$  for tensile strain ( $\epsilon > 0$ ).

We now need to evaluate  $\frac{d\beta}{dD}$ . Butter and Hocker claim that it can be shown that

$$\frac{d\beta}{dD} = \left(\frac{V^3}{2\beta D^3}\right)\frac{db}{dV} \quad (28)$$

where  $\frac{db}{dV}$  is the slope of the  $b - V$  dispersion curve at the point that describes the waveguide mode. Using (17), (18), (21), (26), (27), and (28), we obtain

$$\Delta\phi = \beta\epsilon L + L\frac{d\beta}{dn}\Delta n + L\frac{d\beta}{dD}\Delta D, \quad \text{or} \quad (29)$$

$$\Delta\phi = \beta\epsilon L + Lk_o\left(\frac{-n^3}{2}\right)[\epsilon(1-\mu)P_{12} - \mu\epsilon P_{11}] + L\left(\frac{V^3}{2\beta D^3}\right)\frac{db}{dV}(-\mu\epsilon D) \quad (30)$$

$$\frac{\Delta\phi}{\epsilon L} = \beta - \frac{\beta n^2}{2}[(1-\mu)P_{12} - \mu P_{11}] - \frac{\mu V^3}{2\beta D^2}\frac{db}{dV} \quad (31)$$

Butter and Hocker state that for typical glasses,  $n = 1.5$ ,  $\mu = 0.25$ ,  $P_{11} \approx P_{12} \approx 0.3$ , and that in the single mode region of  $b - V$  dispersion curve,  $V \approx 2.5$  and  $db/dV \approx 0.5$ . With

$D \sim 2 \times 10^{-6}m$  and  $\beta = 1.5 \times 10^7 m^{-1}$ , we obtain

$$\begin{aligned} \frac{\Delta\phi}{\epsilon L} &= 1.5 \times 10^7 m^{-1} - (1.50 \times 10^7 m^{-1})\frac{(1.5)^2}{2}[(1-0.25) \times 0.3 - (0.25) \times 0.3] \quad (32) \\ &\quad - \frac{(0.25)(2.5)^3(0.5)}{2(1.5 \times 10^7 m^{-1})(2 \times 10^{-6})^2} \end{aligned}$$

and

$$\frac{\Delta\phi}{\epsilon L} = 1.5 \times 10^7 m^{-1} - 2.5 \times 10^6 m^{-1} - 1.63 \times 10^4 m^{-1} \approx 1.25 \times 10^7 m^{-1} \quad (33)$$

As Butter and Hocker state, the third term  $1.63 \times 10^4 m^{-1}$  is negligible. It is even more negligible if the mode diameter is larger. They therefore adopt the expression for the phase change per unit stress per unit length as

$$\frac{\Delta\phi}{\epsilon L} = \beta - \frac{\beta n^2}{2} [(1 - \mu)P_{12} - \mu\epsilon P_{11}] = 1.25 \times 10^7 m^{-1} = C_1 \quad (34)$$

By making a round trip through the fiber,  $L$  is effectively doubled. Also, because they used a fiber under tension and a fiber under compression, the relative phase change is doubled. Therefore, the phase difference between the signals traveling through the two fibers is

$$\Delta\phi_{tensile} - \Delta\phi_{compress} = \epsilon(2L)C_1 - ((-\epsilon)(2L)C_1) = 2\epsilon(2L)C_1 \quad (35)$$

then,

$$\Delta\phi_{tensile} - \Delta\phi_{compress} = 2\epsilon(2L)C_1 \quad (36)$$

To see one fringe pass by a reference mark, the relative phase change must be  $2\pi$ . Thus,

$$2\pi = 2\epsilon(2L)C_1 \quad (37)$$

This is for one fringe. Because the strain is dependent on the position  $x$  along the fiber,  $\epsilon$  is replaced by its average value:

$$2\pi = 2\bar{\epsilon}(2L)C_1 \quad (38)$$

The average strain that can be measured by observing one fringe shift is

$$\bar{\epsilon} = \frac{\pi}{2LC_1} = \frac{\pi}{2(0.3)(1.25 \times 10^7 m^{-1})} = 4.19 \times 10^{-7} \quad (39)$$

We note that Thorlabs, the supplier of the bare, single-mode fiber that is glued to the cantilever, could only provide some of the data to characterize the fiber:  $n = 1.459$  and  $V = 2.2796$ . The mode diameter of the fiber is specified to be  $D = 3.6 \times 10^{-6} m$  to  $5.3 \times 10^{-6} m$ .

Our cantilever has width  $b = 2.5$  in, thickness  $2a = 0.25$  in, and length 12 in then we can calculate the average strain:

$$\beta = nk_0 = 1.459 \times \frac{2\pi}{\lambda} = 1.459 \times \frac{2\pi}{6.33 \times 10^{-7}} \approx 1.45 \times 10^7 \text{ m}^{-1}$$

with  $P_{11} = 0.113$  and  $P_{12} = 0.252$  for optical fibers.<sup>12</sup> Then, for one fringe, and core diameter of  $D = 5.3 \times 10^{-6}$  m

$$\begin{aligned} \frac{\Delta\phi}{\epsilon L} &= 1.45 \times 10^7 \text{ m}^{-1} & (40) \\ &- (1.45 \times 10^7 \text{ m}^{-1}) \frac{(1.459)^2}{2} [(1 - 0.25) \times 0.252 - (0.25) \times 0.113] \\ &- \frac{(0.25)(2.2796)^3(0.5)}{2(1.45 \times 10^7 \text{ m}^{-1})(5.3 \times 10^{-6})^2} \approx 1.20 \times 10^7 \text{ m} \end{aligned}$$

$$\bar{\epsilon} = \frac{\pi}{2LC_1} = \frac{\pi}{2(0.3048)(1.20 \times 10^7 \text{ m}^{-1})} \approx 4.28 \times 10^{-7} \quad (15)$$

For a core diameter of  $D = 3.6 \times 10^{-6}$  m,

$$\frac{\Delta\phi}{\epsilon L} \approx 1.20 \times 10^7 \text{ m} \quad (42)$$

Then

$$\bar{\epsilon} \approx 4.28 \times 10^{-7} \quad (43)$$

In both cases we can round the average strain to be

$$\bar{\epsilon} \approx 4.28 \times 10^{-7} \quad (44)$$

## Chapter Three: Methodology and The Optical Alignment

### 1. Methodology

In this chapter, I describe the design, components, construction, and procedure of the experiment. The experiment is, essentially, a modified version of the one performed by Butter and Hocker, as described in Chapter 2. The design for this experiment is shown in Fig. 11.

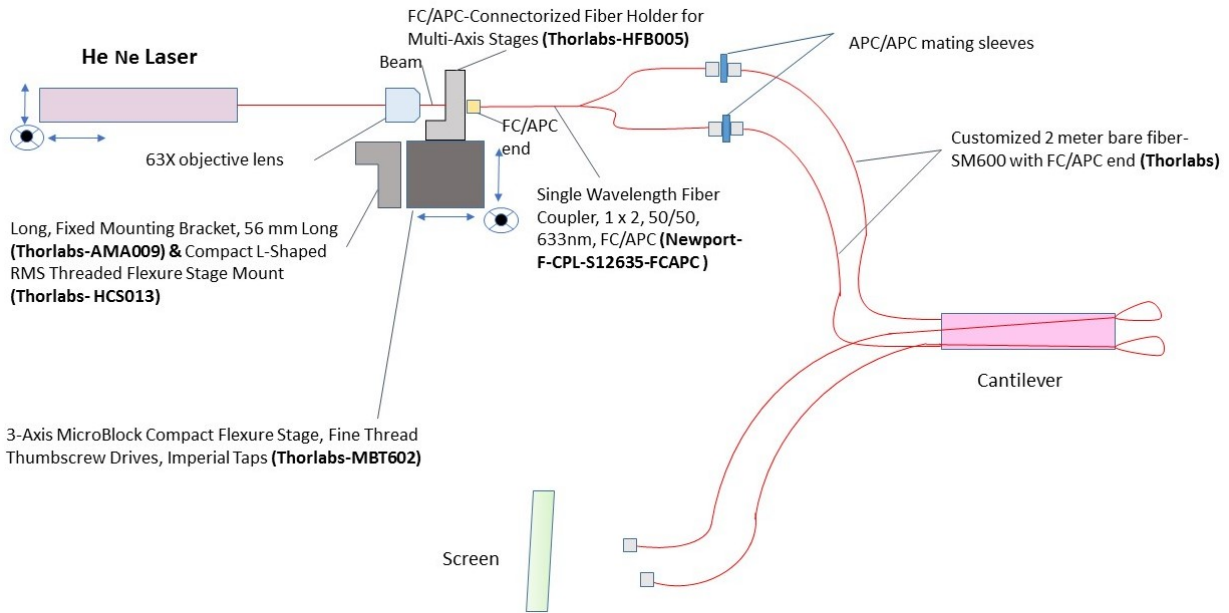


Fig. 11: A schematic diagram of the optical fiber strain gauge.

As Fig. 11 shows, a Melles Griot (05-LHD-991) He-Ne laser<sup>13</sup> that has a wavelength of 633 nm and maximum power of approximately 11 mW served as the beam source. The laser tube is mounted in a tilt stage (Newport ULM-Tilt)<sup>14</sup> that allows two different tilt adjustments. The tilt stage is attached to translation stages that permit motion in the x-, y-, and z- directions. The laser beam is focused by a Melles Griot objective lens<sup>15</sup> that has a magnifying power of  $63\times$  to focus the laser beam onto the end of a Newport fiber coupler.<sup>16</sup> The objective lens is attached to a long, fixed mounting bracket 56 mm (2.20") Mounting Arm (Thorlabs AMA009).<sup>17</sup> The objective lens is mounted in a Compact L-Shaped RMS Threaded Flexure Stage Mount (Thorlabs HCS013).<sup>18</sup>

The bracket is directly attached to a 3-Axis MicroBlock Compact Flexure Stage with Fine Thread Thumbscrew Drives (Thorlabs MBT602).<sup>19</sup> A FC/APC-Connectorized Fiber Holder (Thorlabs HFB005)<sup>20</sup> is also attached to the flexure stage. This fiber holder holds one end of a Single Wavelength Fiber Coupler, 1 x 2, 50/50, 633nm, FC/APC (Newport F-CPL-S12635-FC/APC).<sup>16</sup> The fiber coupler splits the laser beam and allows coupling into two Thorlabs 2 meter bare fiber-SM600 with FC/APC ends.<sup>21</sup> The two bare fibers are glued by epoxy to a 30 cm cantilever. The two input ends of the bare fibers are attached to the fiber coupler by mating sleeves (Thorlabs ADAFC3).<sup>22</sup> The two output ends of the bare fibers are mounted on posts and stands through adapters for each end. A screen was used to monitor the expected interference patterns. A 0.5 in diameter stainless steel mounting post is mounted on a Mitutoyo translation stage with a smallest scale division of 0.0001 inch<sup>23</sup> to displace the end of the cantilever.

## **2. The Optical Alignment**

Coupling the laser into the fiber coupler requires significant care and fine control of the relative positions of the laser, objective, and the end of the fiber coupler. Before attaching the fiber splitter to the holder on the flexure stage, we attached a 1 m, single-mode optical fiber (Thorlabs SM600)<sup>24</sup> to the fiber holder and measured the power transmitted into the fiber. This step helped us to align the fiber holder so that we can simply replace the single-mode fiber with the fiber coupler. Fig. 12 is a photograph of the laser and flexure stage when the single-mode fiber is attached to the fiber holder.

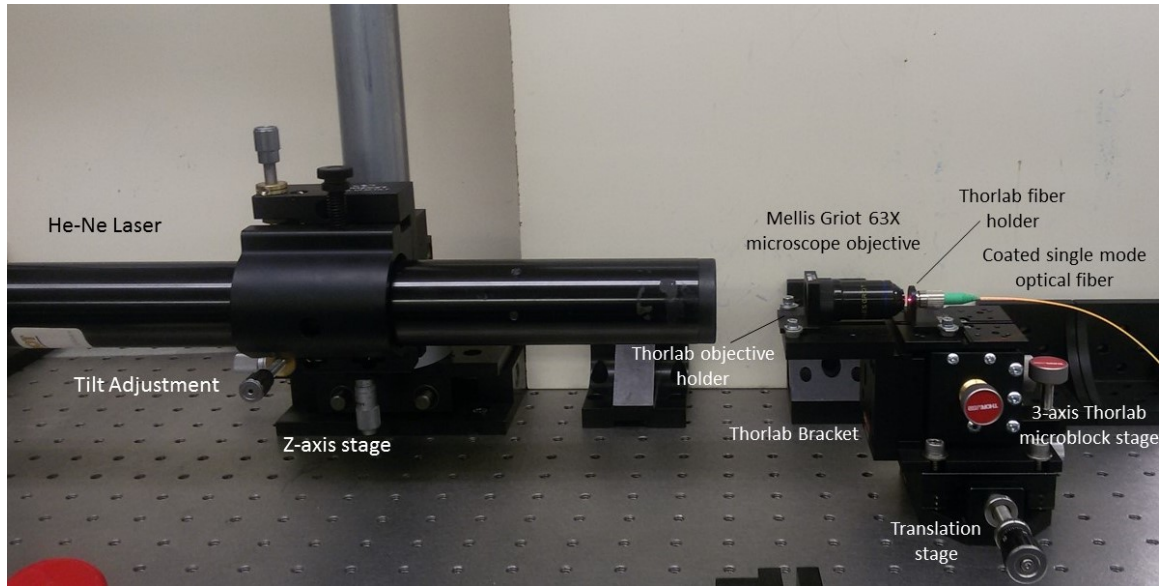


Fig. 12: Setup for optical pre-alignment.

As Fig. 12 illustrates, the laser was mounted on three translation stages. That allowed the laser to move in xyz-directions in addition to the tilting stage that allowed the laser tube to tilt vertically and horizontally (“pitch” and “yaw”). On the other hand, the Thorlabs microblock stage was mounted on a translation stage, which allowed the microblock stage and all attachments to be moved in one direction. After setting all the equipment, the laser beam height was measured as well as the expansion of the beam. This was done to ensure that the laser was not tilted so that the laser beam passed straight through the objective lens and the fiber connector. The objective lens was removed first to ensure that the fiber connector was properly aligned. Now, by placing the objective lens again and moving all equipment relative to the objective lens, the power was maximized and almost perfect alignment was obtained since the transmitted power reached approximately 10 mW.

After the pre-alignment was performed, we started setting up the whole system. The aluminum cantilever is an aluminum plate that is 30 cm long, 10 cm wide, and 0.25 in thick. The cantilever has two shallow grooves, one on each side. The optical fibers were glued into the

grooves. The gluing process required care to avoid breaking the fibers because the fibers were bare fibers with cladding and core only. The glued fibers on the cantilever were left one day to dry. The cantilever was then moved very gently, to avoid damage, to the table. The cantilever was fixed perpendicularly by two Thorlabs brackets that were fixed on the table. In order to apply stress on the cantilever, an optical post mounted on a translation stage was placed in front of the free end of the cantilever. After setting up the cantilever and the fibers, the coated single-mode fiber was replaced by the fiber coupler. The ends of the fiber coupler were connected to the input ends of the two bare fibers by two fiber connectors. The other two ends were mounted on adapters, which were mounted on posts and stands to prevent the motion of the fiber ends. Fig. 13 shows the experimental setup of the apparatus.

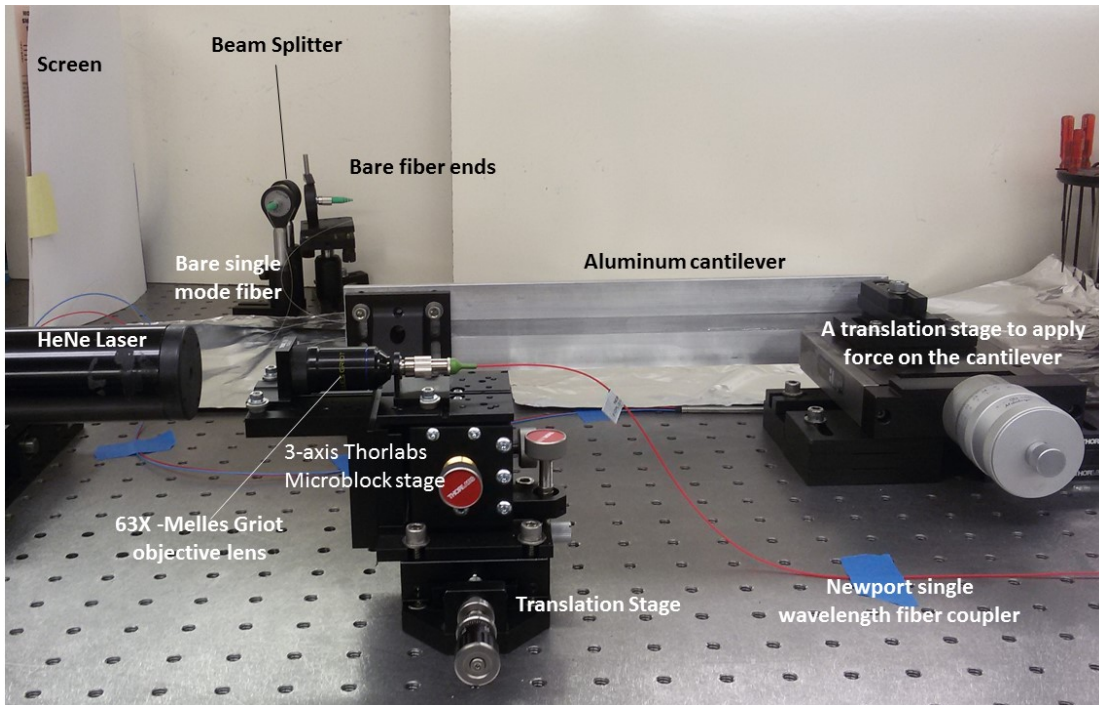


Fig. 13: Setup for the optical fiber strain measurement.

## Chapter Four: Data and Analysis

After finishing the setup, we started the process of seeking interference patterns. We were able to see the laser light transmitted through both ends of the bare fibers. To obtain interference pattern, the light from the ends of the bare fibers was made to overlap. However, we were not able to see any fringes. As a result, the polarization of the laser beam from the laser tube, the polarization of the fiber coupler and the polarization of the fibers were tested. The polarization was examined because if the polarization two beams were mutually perpendicular, then no interference would result. We then connected the fiber coupler outputs directly to the adapters to see if we would be able to get an interference pattern. Although we made sure that the both ends had the same polarization orientation, we were not able to obtain any interference fringes. Then, to get a collinear overlap, we used a plate beam splitter between the two ends, but still no fringes were observed. Then, we connected the bare fibers again to see if we would obtain interference, but the results did not change. Because of time constraints, we decided to calculate theoretically how sensitive the optical strain gauge might be. Second, we measured the beam profile to understand the original beam. Third, we measured the efficiency of the coupling of the free space beam to the fiber. These measurements will be useful for future researchers.

### 1. Sensitivity of Optical Fiber Strain Gauge

In this section, we will compute the sensitivity of the optical fiber strain gauge by using a Python program. We define the sensitivity as the strain required to produce one fringe shift. A detailed description of the code, which was written by Dr. Behringer, is in the APPENDIX section. Basically, this code evaluates (39) from chapter 2. Assuming a mode diameter of  $5.3 * 10^{-6}$  m, we used the Python program to calculate the sensitivity of the strain gauge versus the values of the strain tensor elements  $P_{11}$  and  $P_{12}$ . The plot is shown in Fig. 14.



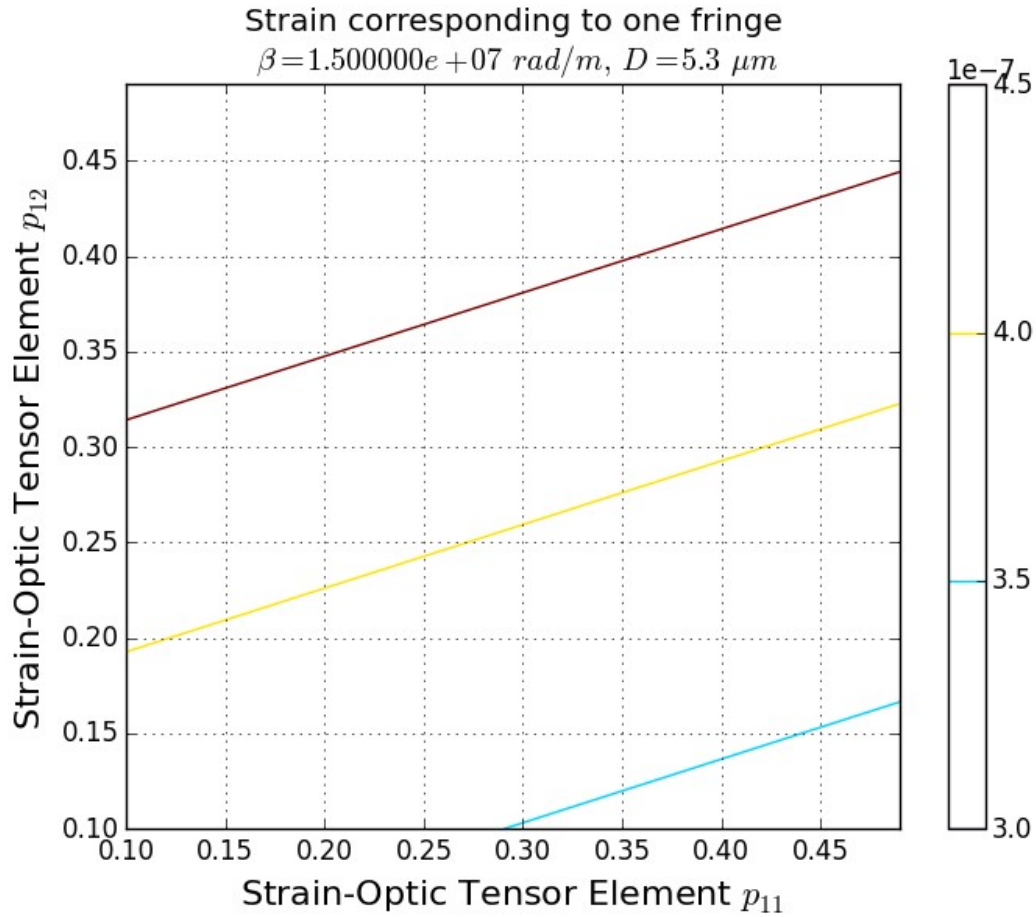


Fig 14: A contour plot of the sensitivity versus strain-optic tensor elements for a fiber mode diameter of 5.3  $\mu\text{m}$ .

The corresponding plot of the sensitivity is shown in Fig. 15, assuming the lower value of the mode diameter of the fiber of 3.6  $\mu\text{m}$ , as quoted by Thorlabs for SM600 fiber.

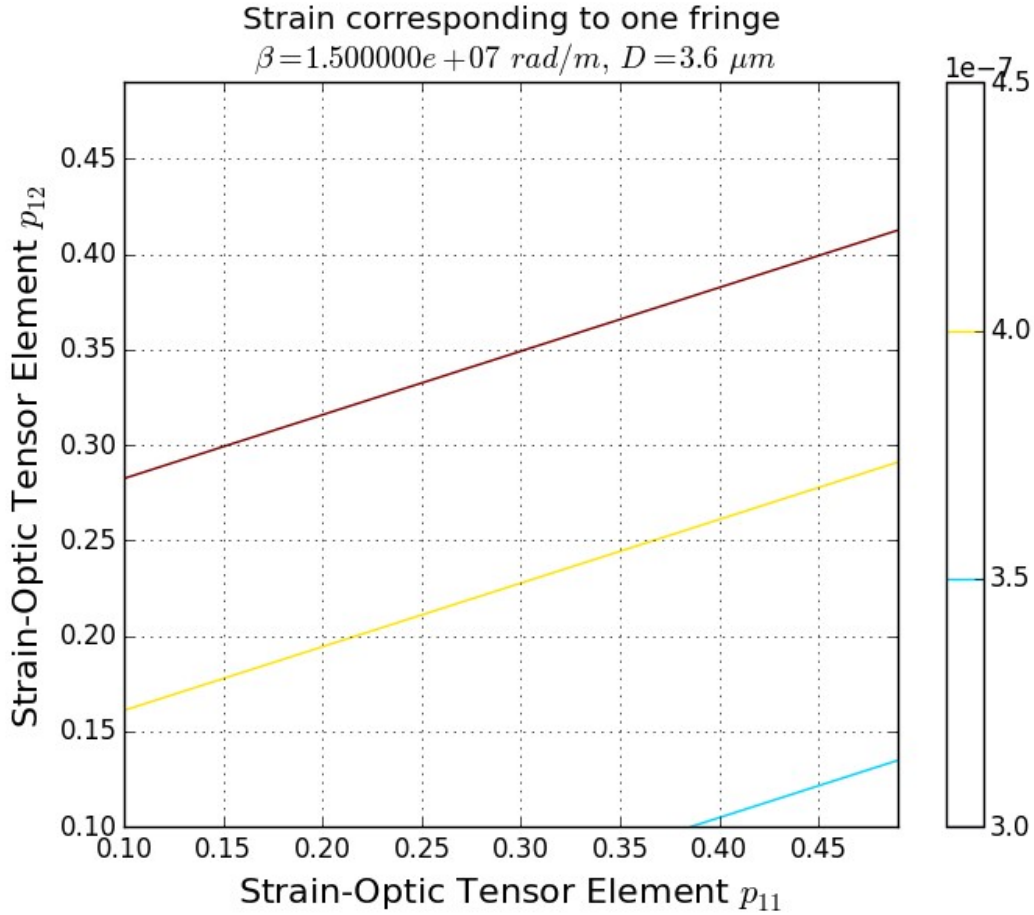


Fig 15: A contour plot of the sensitivity versus strain-optic tensor elements for a fiber mode diameter of  $3.6 \text{ }\mu\text{m}$ .

As seen in Fig. 14 and Fig. 15, the larger mode diameter results in greater sensitivity because the same values of strain-optic tensor elements results in a smaller strain to produce the fringe shift.

## 2. Measuring the Beam Profile

### A. Determination of the Beam Profile Using the Knife-Edge Method:

#### Experimental Method, Data, and Analysis

We used the knife-edge method to determine the beam profile. The method involves translating an opaque knife-edge across the laser beam while measuring the power transmitted

past the knife-edge. Initially, when the knife-edge is far from the beam, the measured power is maximum. Finally, the beam is completely blocked from the detector and the measured power is (ideally) zero. A schematic diagram of the experimental setup is shown in Fig. 16, and a photograph is shown in Fig. 17.

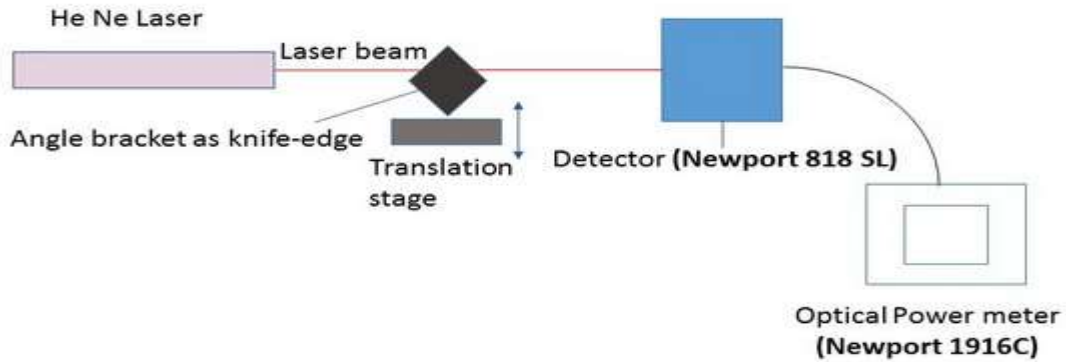


Fig. 16: A schematic diagram of the apparatus for using the knife-edge technique for determining the beam profile.

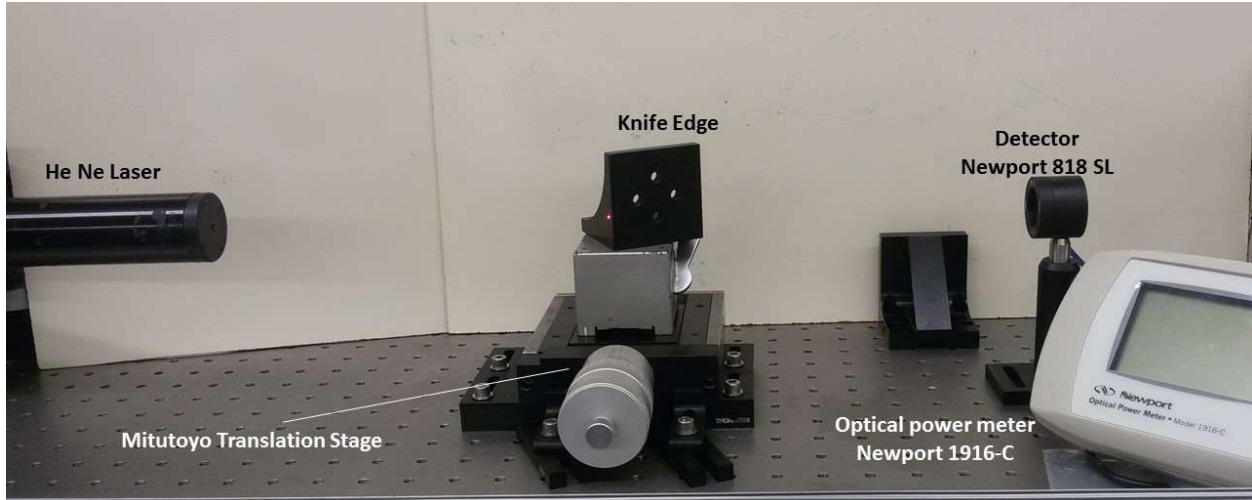


Fig. 17: A photograph of the experimental setup for using the knife-edge technique to determine the beam profile.

A Melles Griot (05-LHD-991) He-Ne laser that has a wavelength of 633 nm served as the beam source.<sup>13</sup> It produced a beam of  $10.780 \text{ mW} \pm 0.020 \text{ mW}$  as measured using a Newport

Model 818 SL Detector together with a Newport Model 1916C Optical Power Meter.<sup>25</sup> The laser was connected to a JDS Uniphase (1202-1) power supply.<sup>26</sup> A Mitutoyo translation stage with a smallest scale division of 0.0001 inch<sup>23</sup> was located in front of the laser and supported a right-angle bracket that served as the knife edge. The stage sat on ThorLabs baseplates and was confined so it does not move.

The measurements we present here were taken with the room lights off. The position of the knife-edge spanned scale readings from 0.3250 to 0.4550 inches and power measurements were recorded after changing the position by  $0.0010 \pm 0.0001$  inch every time until the laser beam was totally blocked. The power meter reading started from  $10.780 \text{ mW} \pm 0.020 \text{ mW}$  and decreased to  $0.000 \text{ mW} \pm 0.026 \text{ mW}$  when the laser beam was totally blocked. After taking the readings, I determined the diameter of the laser beam using the method described by Tiffany Thompson.<sup>27</sup> A plot of the raw power reading versus the raw stage reading  $x$  is shown in Fig. 18.

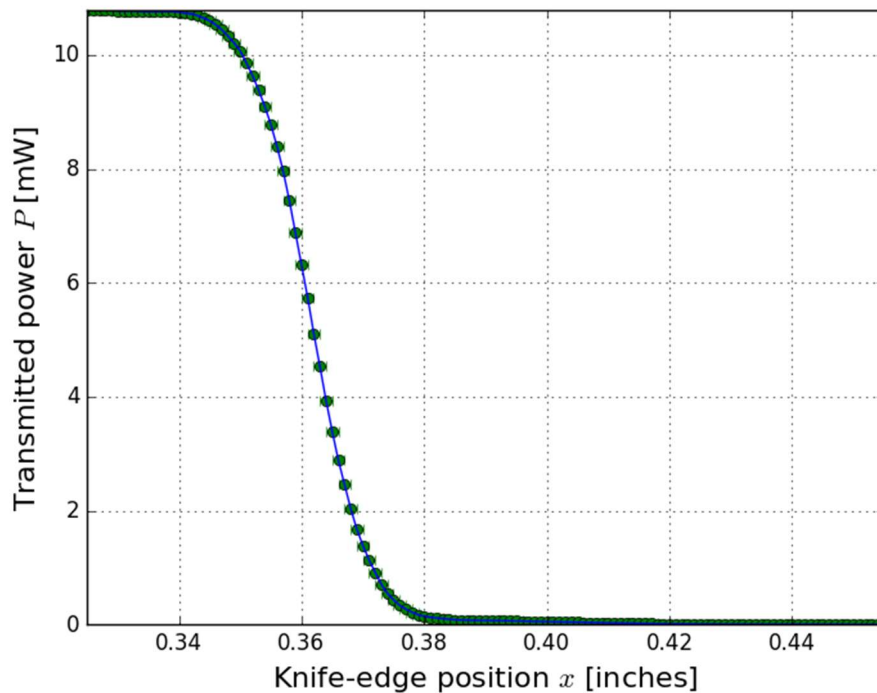


Fig. 18: Plot of the raw power reading versus the raw stage reading.

I calculated  $x_{1/2} - x$  where  $x_{1/2}$  is the position where  $\frac{P(x) - P_{bkgd}}{P_{max}} = 0.5$ , where  $P_{max} = P_{peak} - P_{bkgd}$ .<sup>9</sup>  $P_{bkgd}$  was 0.000 mW,  $P_{peak}$  was about 10.780 mW, and  $P_{max}$ , as a result, was 10.780 mW. A plot of  $\frac{P(x) - P_{bkgd}}{P_{max}}$  versus  $x_{1/2} - x$  is shown below in Fig. 19.

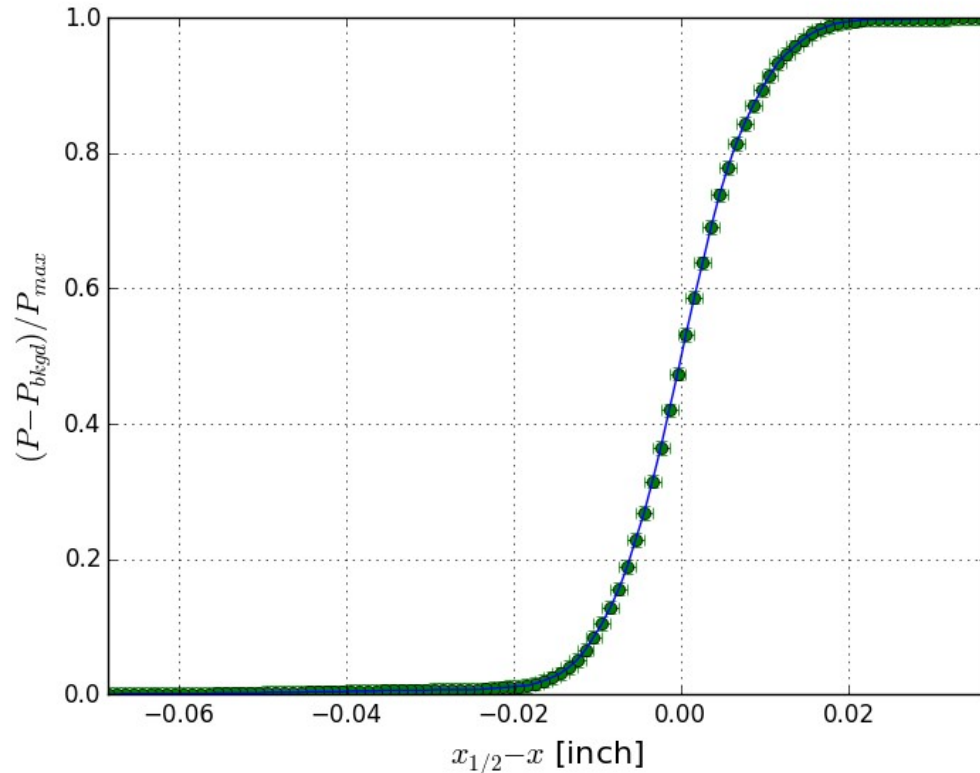


Fig. 19: Plot of  $\frac{P(x) - P_{bkgd}}{P_{max}}$  versus  $x_{1/2} - x$ .

The beam radius was determined using a Python code written by Dr. Ernest Behringer and modified by me. The laser beam radius is  $\frac{w_0}{\sqrt{2}}$  and Fig. 20 shows the plot we generated using the Python program, which performs a least squares fit to the theoretical knife-edge beam profile function. The best value of  $w_0$  is approximately (0.0106) inch.

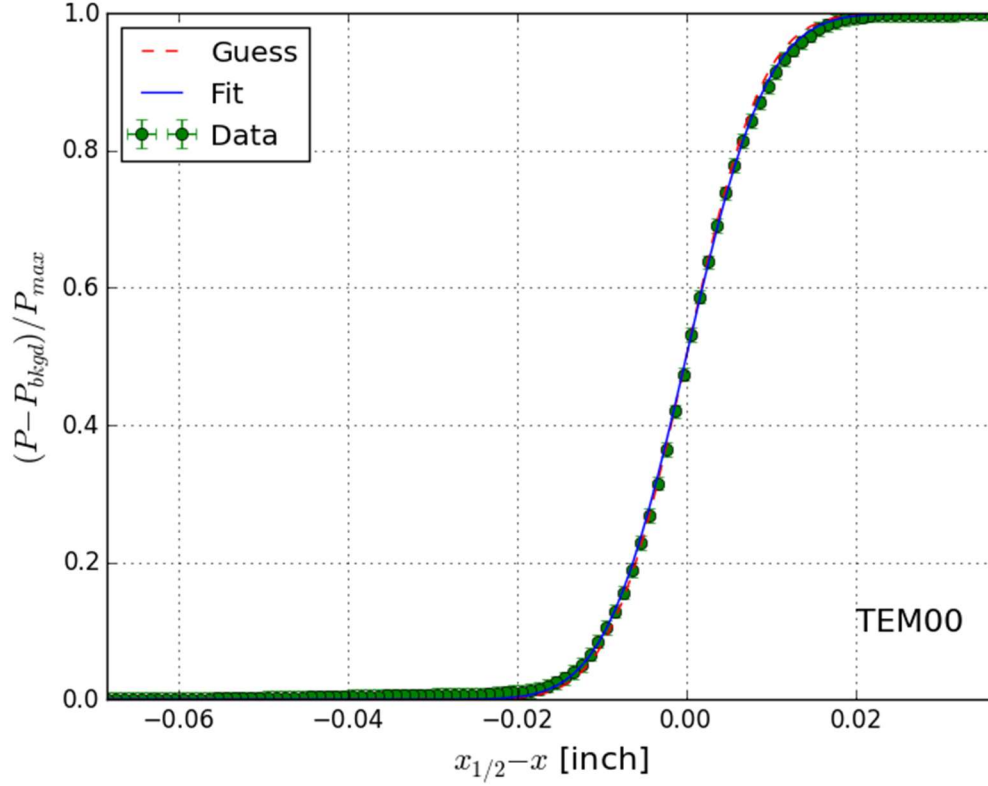


Fig. 20: Plot of  $\frac{P(x)-P_{bkgd}}{P_{max}}$  versus  $x_{1/2} - x$  with the fit function.

The calculations are as follows:

$$\frac{P(x)-P_{bkgd}}{P_{max}} = \frac{1}{2} + \frac{1}{2} \operatorname{erf}\left(\frac{x}{w_0}\right)$$

which can be derived by assuming a Gaussian beam profile for the TEM<sub>00</sub> mode:

$$I(x_{\pm}) = I_{max} e^{-2x^2/w_0^2}$$

$$I(x_{\pm}) = \frac{1}{2} I_{max} \quad \text{then, the radius of the laser beam is}$$

$$x_{\pm} = w_0 \sqrt{\frac{\ln 2}{2}}, \quad \text{which approximately equals to 0.0062 inches or } \approx 0.16 \text{ mm, which gives}$$

us a laser beam diameter of approximately 0.32 mm.

## B. Determination of the Beam Profile Using an Optical Fiber:

### Experimental Method, Data, and Analysis

We used an optical fiber to measure the beam profile. We used the same setup as before, but the knife-edge was replaced by a 1 m, single-mode optical fiber that has a diameter of 3.6–5.3 $\mu\text{m}$  at 633 nm, cladding diameter of 125  $\mu\text{m}$ , 0.13 NA, and FC/APC ends from ThorLabs (SM600).<sup>24</sup> The optical fiber is connected to a 3-axis microblock stage (Thorlabs MBT602)<sup>19</sup> that is mounted on the Mitutoyo horizontal translation stage. The optical fiber was connected to the stage by using a Thorlabs FC/APC-Connectorized Fiber Holder. On the other end, the optical fiber cable was connected to the detector by using a Newport FC/APC Fiber Adapter for 818 & 918D Series Sensors (884-FCA) as shown in Fig. 21 and Fig. 22

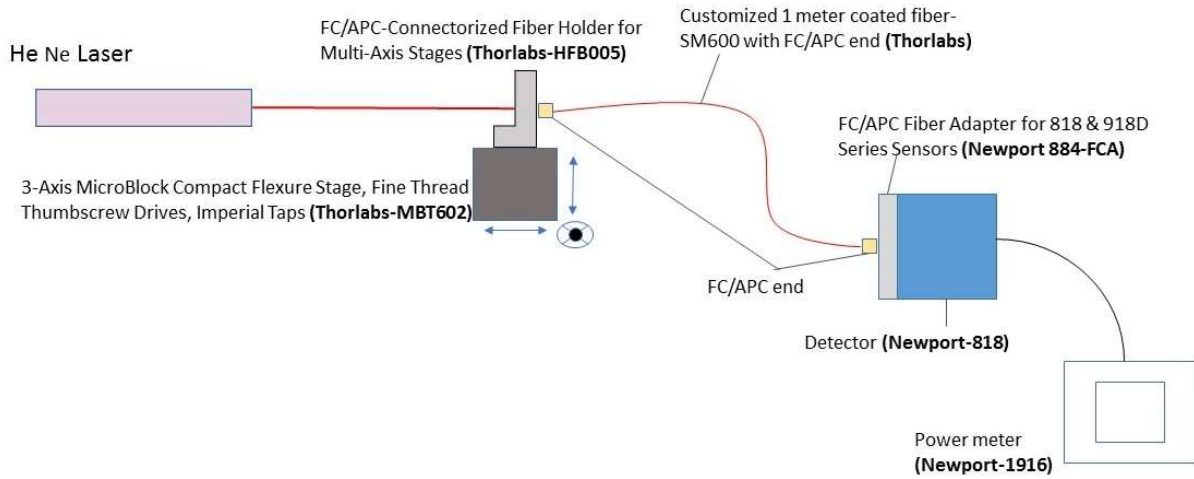


Fig. 21: A schematic diagram of the apparatus for using the single-mode optical fiber to determine the beam profile.

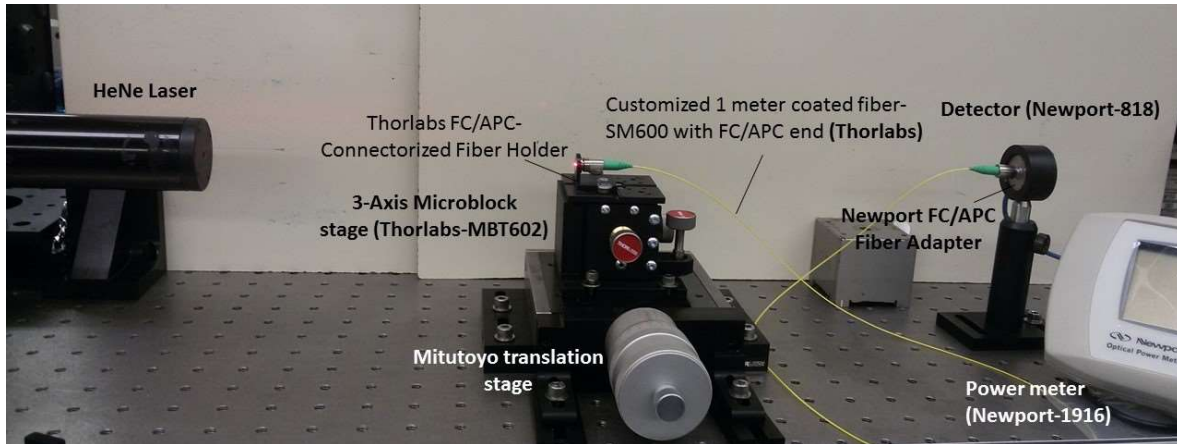


Fig. 22: The apparatus for using the single-mode optical fiber cable for determining the beam profile.

The stage reading started from 0.5250 inches and ended with 0.6100 inches  $\pm$  0.0001 inch until none of the beam hit the fiber. The power data started with approximately 221.4 nW and reached the peak when the detector reading was 1.557 mW  $\pm$  0.003 mW and then decreased to 238.5 nW with uncertainty of 0.1 nW. We used a Python program to plot the data, which are shown in Fig. 23.



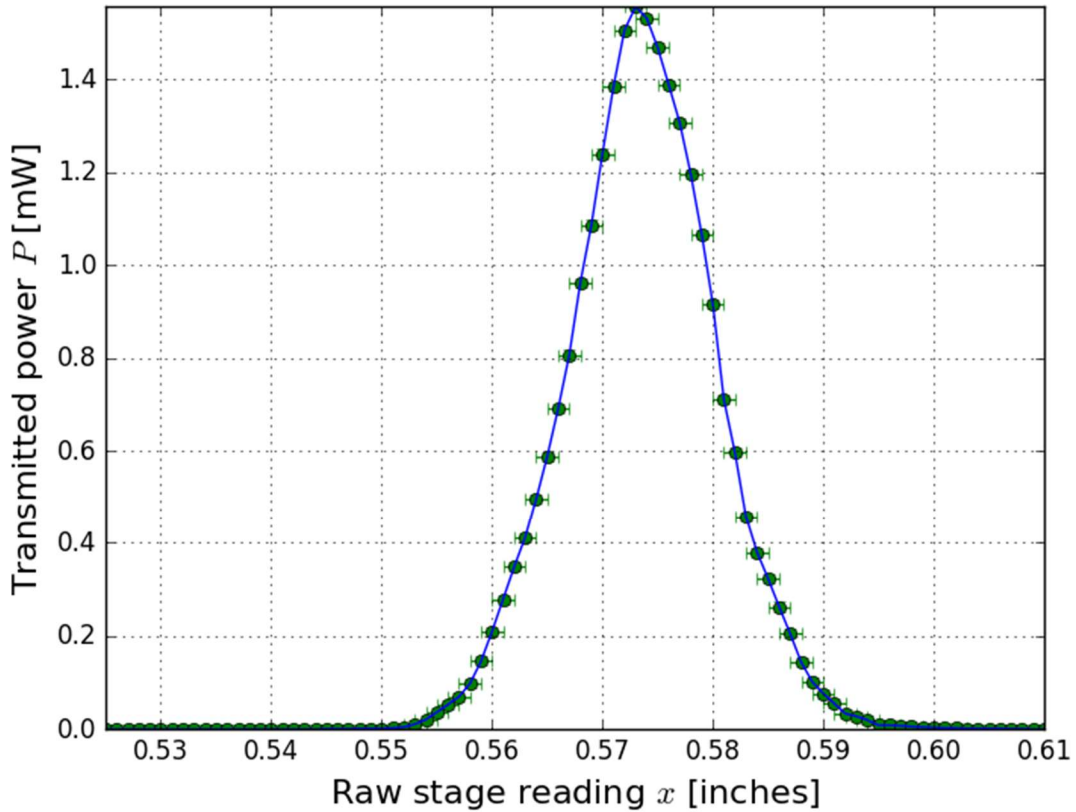


Fig. 23: Plot of the raw stage reading versus the transmitted power.

The measured power was then divided by the maximum power so that the highest value of the resulting scaled power becomes 1.00. Although the room lights were on when these data were taken, there was no background subtraction because there was no change in power reading when the room lights were turned off. After that, another Python program calculated the theoretical beam profile, taking into account the finite radius of the fiber. Figures 24, 25, and 26 compare the measured beam profile from Fig. 23 to the theoretically-predicted beam profile calculated using assuming beam radii  $w$  of 250, 260, and 270  $\mu\text{m}$ , which correspond to beam diameters of 500, 520, and 540  $\mu\text{m}$  respectively.

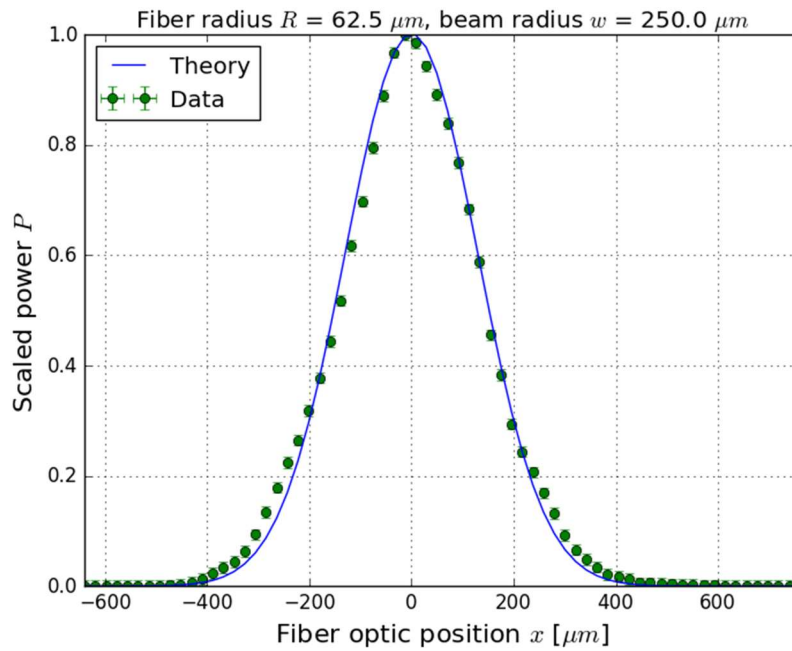


Fig. 24: Comparison of the beam profile measured with the optical fiber to the theoretical beam profile when  $w = 250 \mu m$ .

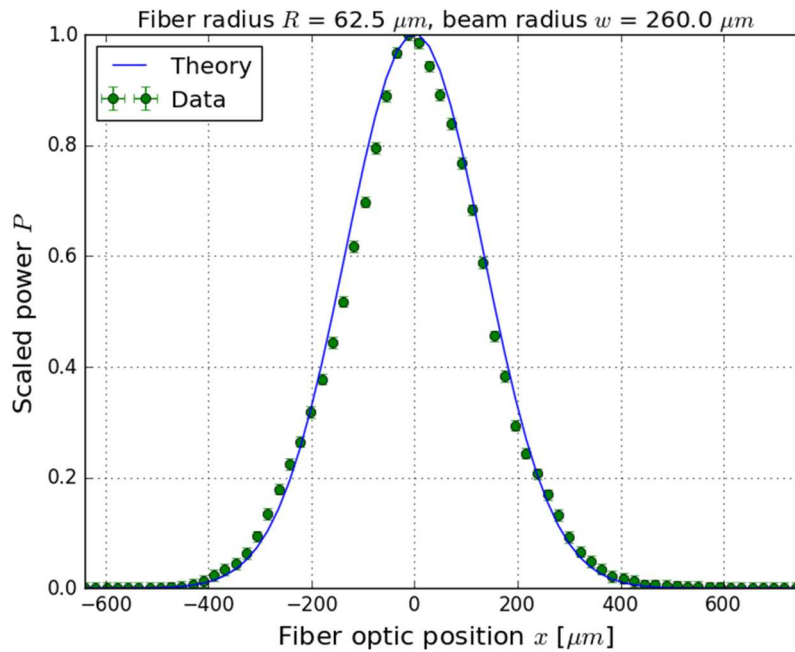


Fig. 25: Comparison of the beam profile measured with the optical fiber to the theoretical beam profile when  $w = 260 \mu m$ .

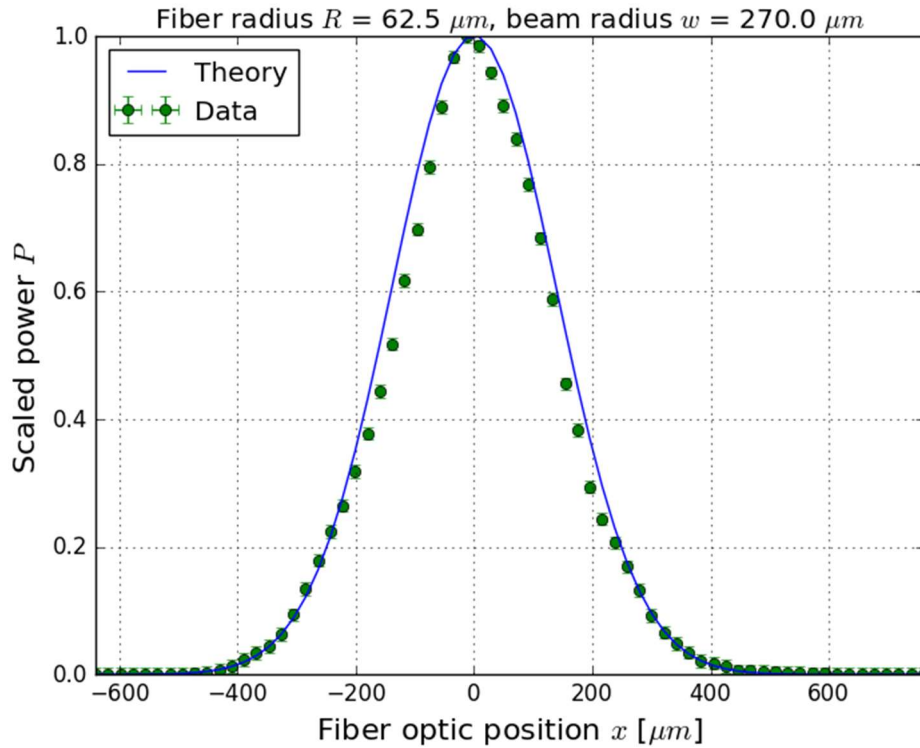


Fig. 26: Comparison of the beam profile measured with the optical fiber to the theoretical beam profile when  $w = 270 \mu m$ .

Although the theoretical beam profiles for these values of  $w$  did not perfectly fit the data, they gave us a sense of the best fit that we could obtain. Now, when we compared the values of the beam diameter obtained by using optical fiber with the beam diameter obtained by knife-edge, we saw that they do not match. In fact, we realized that the beam diameter obtained by using the fiber was approximately twice the beam diameter obtained by using the knife-edge.

### 3. Measuring the Efficiency of Coupling the Free Space Beam to the Fiber:

#### Experimental Method, Data, and Analysis

In order to see how sensitive the coupling of the free space laser to a fiber can be, we used the same fiber we used to measure the beam profile. The setup was similar to the beam profile setup, but we changed the direction of the translation. We also used a Thorlab 4X

objective lens (RMS4X)<sup>28</sup> to focus the laser beam into the fiber. The laser beam was directed to the Thorlab 4X objective lens, which was mounted on a stand. The objective lens focused the laser beam into a single-mode optical fiber (ThorLabs SM600).<sup>24</sup> The optical fiber was attached to a FC/APC-Connectorized Fiber Holder (Thorlabs HFB005)<sup>20</sup> which was mounted on the 3-axis Thorlabs microblock translation stage. The microblock stage was fixed on a z-axis Mitutoyo translation stage. The other end of the optical fiber was connected to the detector by using a Newport FC/APC Fiber Adapter for 818 & 918D Series Sensors (884-FCA) as shown in Fig. 27 and Fig. 28

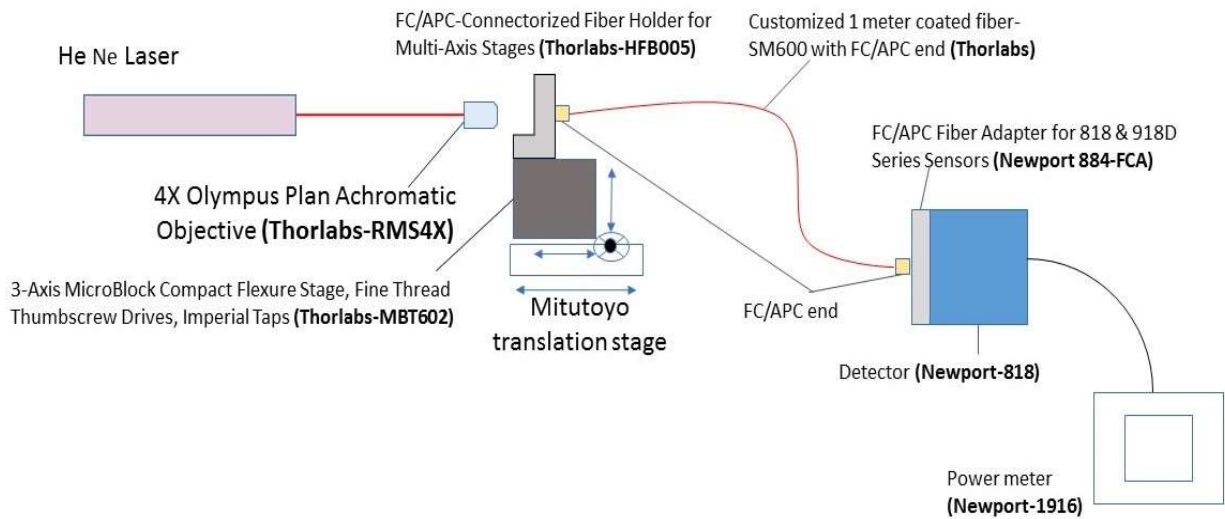


Fig. 27: A schematic diagram of the apparatus for measuring the sensitivity of the coupling of the free space beam to the fiber.

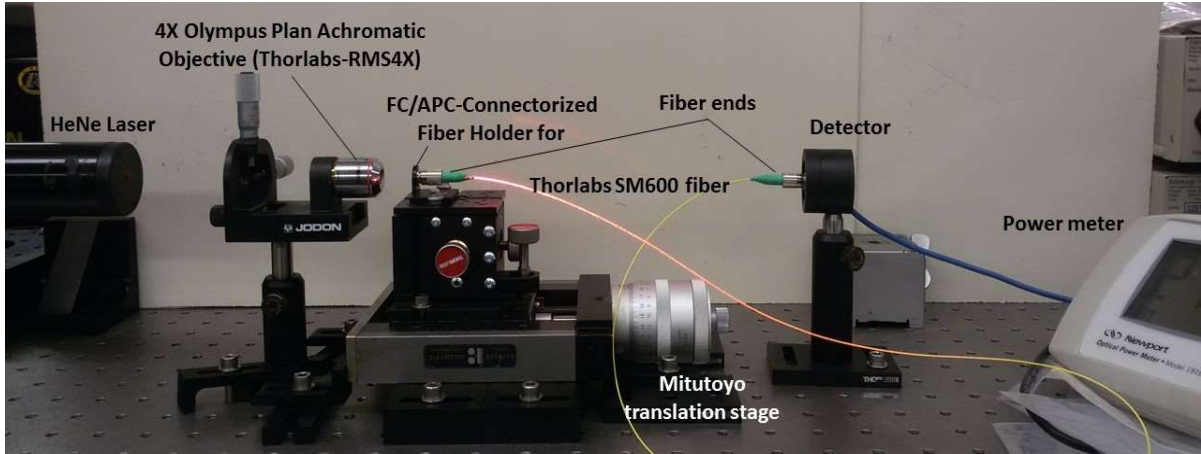


Fig. 28: The apparatus for measuring the sensitivity of the coupling of the free space beam to the fiber.

Again, a maximum transmitted power of  $218.5 \mu\text{W}$  was obtained before taking the data. The process of taking data is exactly similar to the beam profile. The only difference in this experiment was moving the fiber closer to and farther from the objective. The stage reading started from  $0.1580 \text{ in}$  and ended with  $0.2210 \text{ in} \pm 0.0001 \text{ in}$ , and power measurements were recorded after changing the position by  $0.0005 \pm 0.0001 \text{ in}$  every time. We started the power data from approximately  $199.7 \mu\text{W} \pm 0.1 \mu\text{W}$  and reached the peak when the detector reading was  $218.5 \mu\text{W} \pm 0.02 \mu\text{W}$  and then decreased to  $199.7 \mu\text{W}$  with uncertainty of  $0.1 \mu\text{W}$ . We used a Python program to plot the data as shown in Fig. 29.

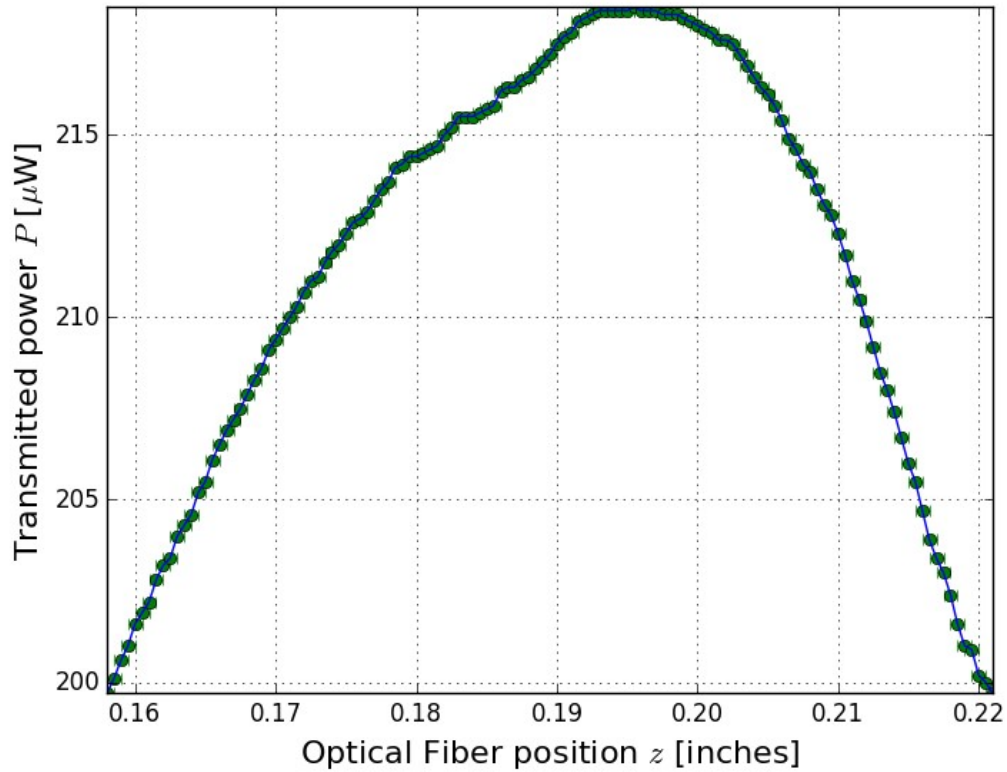


Fig. 29: Fiber coupling sensitivity.

As can be seen from Fig. 29, when the fiber was moved closer to the objective, the power increased then it reached maximum. Now, when the fiber was moved even closer, we saw that the power was decreasing faster than the part where it was increasing. The distance between the fiber and the objective to obtain maximum power depends on the focal length of the objective. It might not be shown explicitly in Fig. 29, but once the power reaches its maximum value, it becomes so sensitive that with a very simple touch, the power decreases. For this reason, I include here a portion of the data table.

Stage [in]	Power [ $\mu$ W]
0.1910	217.8
0.1915	218.1
0.1920	218.2
0.1925	218.3
0.1930	218.4
0.1935	218.4
0.1940	218.4
0.1945	218.4
0.1950	218.4
0.1955	218.5
0.1960	218.4
0.1965	218.4
0.1970	218.4
0.1975	218.3
0.1980	218.3
0.1985	218.3
0.1990	218.2
0.1995	218.1
0.2000	218.0
0.2005	217.9
0.2010	217.8

Table 1: Power versus stage readings for fiber coupling sensitivity.

## Chapter Five: Summary

This project was an attempt to reconstruct the optical fiber strain gauge described by Butter and Hocker. A modified version of the apparatus was built, but no interference pattern resulted when overlapping the two beams transmitted through the two bare optical fibers. The idea was to measure the shift in the interference pattern as a function of the applied force on the cantilever. Unfortunately, because we had a limited time and because we did not observe any interference pattern, we were not able to accomplish our goal to measure strain. We have performed calculations and measurements that will help this project to succeed in the future. These calculations included using a Python code to compute the expected sensitivity of the optical fiber strain gauge. We also measured the beam profile using two methods: the knife-edge method and the optical fiber method. Finally, we measured the sensitivity of the coupling of the free space beam to the fiber. These measurements will help future researchers to modify the gauge so that it produces interference fringes. By calculating the optical fiber strain gauge sensitivity theoretically, we establish the expected sensitivity of the strain gauge. By measuring the beam profile, we have established the diameter of the free space beam. Finally, by measuring the sensitivity of the coupling of the free space beam to the fiber, we give future researchers data about the difficulty of “launching the fiber”.

For future researcher, I suggest to changing the objective lens that was used in the experiment to improve the likelihood of obtaining interference fringes. The reason is that the objective lens that was used in the experiment was not clean. Consequently, the resulting wavefront was not spherical and led to having a very faint interference pattern that couldnot be observed.



## References

- <sup>1</sup> Hong-Nan Li, Dong-Sheng Li, and Gang-Bing Song, J. ENG STRUCT. **26**, 1647 (2004).
- <sup>2</sup> Omega.com manual, <http://www.omega.com/literature/transactions/volume3/strain.html>.
- <sup>3</sup> Omega rectangular 3-element rosette planar compact geometry (SGD-1/120-RY21), [http://www.omega.com/pptst/SGD\\_3-ELEMENT45.html](http://www.omega.com/pptst/SGD_3-ELEMENT45.html).
- <sup>4</sup> Omega.com, practical strain gage measurements, [http://www.omega.com/techref/pdf/StrainGage\\_Measurement.pdf](http://www.omega.com/techref/pdf/StrainGage_Measurement.pdf).
- <sup>5</sup> C. D. Butter and G. B. Hocker. J. Appl. Opt. **17**, 2867 (1978).
- <sup>6</sup> J. M. Gere and B. J. Goodno, Mechanics of Materials, 8th ed. (Cengage Learning, Stamford, Ct, USA, 2012). pp. 2-118.
- <sup>7</sup> K. T. V. Grattan and Dr. T. Sun, J. Sens. Actuators, A. **82**, 40 (2000).
- <sup>8</sup> G. Meltz, W. H. Glenn and E. Snitzer, U. S. Patent No. 4,761,073 (2 August 1988).
- <sup>9</sup> Juan A. Pomarico, Enrique E. Sicre, Dante Patrignani and Lorenzo De Pasquale, J. OPT LASER TECHNOL. **31**, 219 (1999).
- <sup>10</sup> Francisco J. Arregui, Ignacio R. Matias and Manuel Lopez-Amo, J. Sens. Actuators, A. **79**, 91 (2000).
- <sup>11</sup> Mingzheng Jiang and Edmund Gerhard, J. Sens. Actuators, A. **88**, 41 (2001).
- <sup>12</sup> Lars Hoffmann , Mathias S. Müllera, Sebastian Krämerb, Matthias Giebelc, Günther Schwotzerc , and Torsten Wieduwilte. J. Proc. Estonian Acad. Sci. Eng. **13**, 363 (2007).
- <sup>13</sup> (05-LHD-991) He-Ne laser, mellesgriot, <http://mellesgriot.com>.
- <sup>14</sup> (ULM-Tilt) Cylindrical Laser Mount, 1.0-1.75 in., High-Resolution AJS Adjusters, Newport, <http://search.newport.com/?x2=sku&q2=ULM-TILT>.
- <sup>15</sup> (63X) objective lens, Newport, <http://www.newport.com/> .

- 
- <sup>16</sup> (F-CPL-S12635) Single Wavelength Fiber Coupler, 1 x 2, 50/50, 633nm, Newport,  
[http://search.newport.com/?q=\\*&x2=sku&q2=F-CPL-S12635](http://search.newport.com/?q=*&x2=sku&q2=F-CPL-S12635) .
- <sup>17</sup> (AMA009) Long, Fixed Mounting Bracket, 56 mm Long, Thorlabs,  
[www.thorlabs.com/thorproduct.cfm?partnumber=AMA009](http://www.thorlabs.com/thorproduct.cfm?partnumber=AMA009).
- <sup>18</sup> (HCS013) RMS-Threaded Flexure Stage Mount, Thorlabs,  
<http://www.thorlabs.com/thorproduct.cfm?partnumber=HCS013> .
- <sup>19</sup> (MBT602) 3-Axis MicroBlock Compact Flexure Stage, Fine Thread Thumbscrew Drives,  
Imperial Taps, Thorlabs, <http://www.thorlabs.com/thorproduct.cfm?partnumber=MBT602> .
- <sup>20</sup> (HFB005) FC/APC-Connectorized Fiber Holder for Multi-Axis Stages, Thorlabs,  
<http://www.thorlabs.com/thorproduct.cfm?partnumber=HFB005> .
- <sup>21</sup> (SM600) customized two meter bare single mode optical fiber with FC/APC ends, Thorlabs,  
<https://www.thorlabs.com/> .
- <sup>22</sup> (ADAFC3) FC/APC to FC/APC Mating Sleeve, Narrow Key (2.0 mm), Square Flange,  
Thorlabs, <https://www.thorlabs.com/thorproduct.cfm?partnumber=ADAFC3> .
- <sup>23</sup> Mitutoyo translation stage with a smallest scale division of 0.0001 inch, Mitutoyo Corporation,  
<http://www.mitutoyo.com>.
- <sup>24</sup> (SM600) customized one meter single-mode optical fiber with FC/APC end, ThorLabs,  
<https://www.thorlabs.com/> .
- <sup>25</sup> SL Detector, Model 818 and Newport Optical Power Meter, Model 1916C, Newport  
Corporation, <http://www.newport.com>.
- <sup>26</sup> JDS Uniphase (1202-1) power supply, JDSU, <http://www.jdsu.com/en-us/Pages/Home.aspx>.
- <sup>27</sup> T. C. Thompson, M.S. research project, Eastern Michigan University, 2011.

---

<sup>28</sup> (RMS4X) 4X Olympus Plan Achromat Objective, 0.10 NA, 18.5 mm WD, Thorlabs,

<http://www.thorlabs.com/thorproduct.cfm?partnumber=RMS4X>.

---

## APPENDIX A: PYTHON CODES

### a. PYTHON CODE FOR CALCULATING THE STRAIN GAUGE SENSITIVITY

```
#
# Optical_Strain_Gauge_Sensitivity_plot_v3.py
#
# This program generates a contour plot showing
# contours for sensitivity
# as a function of different parameters
# characterizing the cantilever optical strain gauge.
#
# Written by:
#
# Ernest R. Behringer
# Department of Physics and Astronomy
# Eastern Michigan University
# Ypsilanti, MI 48197
# (734) 487-8799
# ebehringe@emich.edu
#
# 20160325 by ERB
#

# import the commands needed to make the plot
from pylab import
xlabel, ylabel, show, colorbar, figure, title, contour, grid

# import the command needed to make a 1D array
from numpy import arange, meshgrid, pi

# input parameters
mu = 0.25 # Poisson's ratio for the fiber
n = 1.459 # index of refraction of the fiber
a = 0.5*0.25*2.54e-2 # half the thickness of the cantilever [m]
b = 2.5*2.54e-2 # width of the cantilever [m]
V = 2.2796 # value of fiber parameter V
dbdV = 0.5 # value of b-V dispersion curve at the mode
L = 0.30 # cantilever length [m]
D = 5.30e-6 # value of the mode diameter of the fiber [m]
#D = 3.60e-7 # Lower value of mode diameter quoted by Thorlabs
for SM600 fiber [m]
D_um = D*1.0e6 # value of the mode diameter of the fiber [um]
#D_um = D*1.0e7
beta = 1.5e7 # propagation constant [rad/m]
```

---

```

# interval and endpoints for the different parameters
# first, the propagation constant
p11_low = .10 # low value of propagation constant [rad/m]
p11_high = .50 # high value of propagation constant [rad/m]
delta_p11 = 0.01 # interval of propagation constant [rad/m]
# second, the strain-optic tensor elements, assuming p11 = p12
p12_low = 0.10 # low value of mode diameter [m]
p12_high = 0.50 # high value of mode diameter [m]
delta_p12 = 0.01 # interval of mode diameter [m]

p11_1D = arange(p11_low,p11_high,delta_p11) # p11 data point
array
p12_1D = arange(p12_low,p12_high,delta_p12) # p12 data point
array

print "len(p11_1D) = ", len(p11_1D)
print "len(p12_1D) = ", len(p12_1D)

# create the grid of values on which the period will be
evaluated
p11, p12 = meshgrid(p11_1D,p12_1D)

# calculate phase change per unit strain per unit length
term1 = beta
term2 = -0.5*beta*n*n*((1.0-mu)*p12 - mu*p11)
term3 = -0.5*mu*V*V*V*dbdV/(beta*D*D)
C1 = term1 + term2 + term3

# calculate the strain that corresponds to a single fringe
shift
strain_one_fringe = 0.5*pi/(L*C1)

# make a contour plot of the speed vs Apar and Aperp
figure()
# specify contour levels
levels = arange(3.00e-7,5.00e-7,0.5e-7)
contour(p11,p12,strain_one_fringe,levels)
#title("Strain corresponding to one fringe, $\beta = %s \, \, n
D = %s \, \, \mu m$"%(beta,D_um))
title("Strain corresponding to one fringe \n $\beta = %e \, \,
rad/m, \, \, D = %s \, \, \mu m$"%(beta,D_um))
xlabel("Strain-Optic Tensor Element $p_{11}$",size=16)
ylabel("Strain-Optic Tensor Element $p_{12}$",size=16)
grid()
colorbar()
show()

```

---

b. PYTHON CODE FOR PLOTTING THE RAW POWER AND STAGE READINGS FOR  
THE BEAM PROFILE—KNIFE-EDGE METHOD

```
#
#
PHY692_Plot_Of_Power_And_Stage_Raw_Readings_For_Laser_TEM00_Mode.py
#
# This file will generate a plot of
# the raw power reading versus the raw stage reading
# for laser TEM00 mode by the knife-edge method
#
# Written by:
#
# Ernest R. Behringer
# Department of Physics and Astronomy
# Eastern Michigan University
# Ypsilanti, MI 48197
# (734) 487-8799
# ebehringe@emich.edu
#
# 20150127 by ERB
#
# Modified by:
# Najwa Sulaiman
# Department of Physics and Astronomy
# Eastern Michigan University
# Ypsilanti, MI 48197
# nsulaima@emich.edu
#
# 20150624 by NS
# 20150716 by NS
# 20150823 by NS
# 20160313 by NS
#
import pylab as p
import numpy as np

X_Points = np.linspace(0.3250, 0.4550, 131)
P_Points = [10.780, 10.780, 10.780, 10.780, 10.780, 10.770,
10.770, 10.770, 10.770, 10.760, 10.760, 10.760, 10.760, 10.760,
10.760, 10.750, 10.730, 10.720, 10.690, 10.650, 10.600, 10.530,
10.440, 10.330, 10.210, 10.070, 9.860, 9.640, 9.380, 9.100,
8.775, 8.396, 7.961, 7.450, 6.882, 6.326, 5.740, 5.107, 4.529,
3.932, 3.392, 2.885, 2.467, 2.042, 1.678, 1.391, 1.135, 0.919,
```

```

0.707, 0.551, 0.434, 0.338, 0.270, 0.217, 0.173, 0.144, 0.128,
0.116, 0.103, 0.094, 0.084, 0.079, 0.076, 0.074, 0.073, 0.072,
0.071, 0.069, 0.067, 0.065, 0.063, 0.061, 0.060, 0.057, 0.054,
0.053, 0.050, 0.048, 0.046, 0.043, 0.040, 0.038, 0.036, 0.033,
0.032, 0.029, 0.027, 0.025, 0.024, 0.022, 0.020, 0.018, 0.017,
0.015, 0.014, 0.012, 0.011, 0.010, 0.009, 0.008, 0.008, 0.007,
0.006, 0.006, 0.005, 0.005, 0.004, 0.004, 0.004, 0.003, 0.003,
0.003, 0.003, 0.003, 0.002, 0.002, 0.002, 0.002, 0.002, 0.002,
0.002, 0.002, 0.001, 0.001, 0.001, 0.001, 0.001, 0.000, 0.000,
0.000, 0.000]
p.xlim(min(X_Points),max(X_Points))
p.ylim(min(P_Points),max(P_Points))

# Error bar data here
X_points_err = 0.001*p.ones(len(X_Points))
Powercorr_points_err = 0.01*p.ones(len(P_Points))

p.xlabel("Knife-edge position $x$ [inches]", size = 16)
p.ylabel("Transmitted power $P$ [mW]", size = 16)
p.grid(True)
p.errorbar(X_Points,P_Points,xerr=X_points_err,yerr=Powercorr_
points_err,fmt="go")
p.plot(X_Points,P_Points,"b")
p.show()

```

c. PYTHON CODE FOR PLOTTING THE CORRECTED POWER AND STAGE

READINGS FOR THE BEAM PROFILE—KNIFE-EDGE METHOD

```

#
#PHY692_Plot_Of_Corrected_Power_And_Stage_Readings_For_TEM00_M
ode_KE.py
#
# This file will generate a plot of
# the modified power reading versus the modified stage reading
# for TEM00 laser mode
#
# Written by:
#
# Ernest R. Behringer
# Department of Physics and Astronomy
# Eastern Michigan University
# Ypsilanti, MI 48197
# (734) 487-8799
# ebehringe@emich.edu
#

```

---

```

# 20150127 by ERB
#
# Modified by:
# Najwa Sulaiman
# Department of Physics and Astronomy
# Eastern Michigan University
# Ypsilanti, MI 48197
# nsulaima@emich.edu
#
# 20150624 by NS
# 20150824 by NS
# 20160313 by NS
#
import pylab as p
import numpy as np

X_mod = np.linspace(0.0366, -0.0684, 106)
P_mod = [1.000, 1.000, 1.000, 1.000, 1.000, 0.999, 0.999,
0.999, 0.999, 0.998, 0.998, 0.998, 0.998, 0.998, 0.998, 0.998, 0.997,
0.995, 0.994, 0.992, 0.988, 0.983, 0.977, 0.968, 0.958, 0.947,
0.934, 0.915, 0.894, 0.870, 0.844, 0.814, 0.779, 0.738, 0.691,
0.638, 0.587, 0.532, 0.474, 0.420, 0.365, 0.315, 0.268, 0.229,
0.189, 0.156, 0.129, 0.105, 0.085, 0.066, 0.051, 0.040, 0.031,
0.025, 0.020, 0.016, 0.013, 0.012, 0.011, 0.010, 0.009, 0.008,
0.007, 0.007, 0.007, 0.007, 0.007, 0.007, 0.006, 0.006, 0.006,
0.006, 0.006, 0.006, 0.005, 0.005, 0.005, 0.005, 0.004, 0.004,
0.004, 0.004, 0.004, 0.003, 0.003, 0.003, 0.003, 0.003, 0.002,
0.002, 0.002, 0.002, 0.002, 0.002, 0.001, 0.001, 0.001, 0.001,
0.001, 0.001, 0.001, 0.001, 0.001, 0.001, 0.000, 0.000]

# Error bar data here
X_points_err = 0.001*p.ones(len(X_mod))
Powercorr_points_err = 0.01*p.ones(len(P_mod))

p.xlim(min(X_mod),max(X_mod))
p.ylim(min(P_mod),max(P_mod))

p.xlabel("$x_{1/2}$-x$ [inch]", size = 16)
p.ylabel("$\frac{P-P_{\text{bkgd}}}{P_{\text{max}}}$", size = 16)
p.grid(True)
p.errorbar(X_mod,P_mod,xerr=X_points_err,yerr=Powercorr_points_err,fmt="go")
p.plot(X_mod,P_mod,"b")
p.show()

```



---

d. PYTHON CODE FOR EVALUATING THE LASER BEAM DIAMETER FOR BEAM  
PROFILE—KNIFE-EDGE METHOD

```
#
# PHY692_Beam_Profile_Analysis_TEM00_KE.py
#
# This file will generate a plot of
# beam profile data and fit function
# for TEM00 laser mode
#
# Written by:
#
# Ernest R. Behringer
# Department of Physics and Astronomy
# Eastern Michigan University
# Ypsilanti, MI 48197
# (734) 487-8799
# ebehringe@emich.edu
#
# Najwa Sulaiman
# Department of Physics and Astronomy
# Eastern Michigan University
# Ypsilanti, MI 48197
# nsulaima@emich.edu
#
# 20150128 by ERB
# 20150506 by NS
# 20150824 by NS
# 20160313 by NS
#
# import the commands needed to make the plot and fit the data
from pylab import
xlim,xlabel,ylim,ylabel,grid,show,plot,legend
from numpy import linspace,ones
from scipy.special import erf
from scipy.optimize import leastsq
from matplotlib.pyplot import errorbar

# Input your data.
# This is not so bad if you don't have much data.
# Here, the first array will be the independent variable
# and the second array will be the dependent variable.

#
# Initialize the vector of parameters
```

---

```

w0 = 0.01 # The initial guess for w0
print(w0)
#
# Noisy 'data' generated here.
# Xcorr is the independent variable.
# Powercorr is the dependent variable.
Xcorr_points = linspace(0.0366, -0.0684, 106)
Powercorr_points = [1.000, 1.000, 1.000, 1.000, 1.000, 0.999,
0.999, 0.999, 0.999, 0.998, 0.998, 0.998, 0.998, 0.998, 0.998,
0.997, 0.995, 0.994, 0.992, 0.988, 0.983, 0.977, 0.968, 0.958,
0.947, 0.934, 0.915, 0.894, 0.870, 0.844, 0.814, 0.779, 0.738,
0.691, 0.638, 0.587, 0.532, 0.474, 0.420, 0.365, 0.315, 0.268,
0.229, 0.189, 0.156, 0.129, 0.105, 0.085, 0.066, 0.051, 0.040,
0.031, 0.025, 0.020, 0.016, 0.013, 0.012, 0.011, 0.010, 0.009,
0.008, 0.007, 0.007, 0.007, 0.007, 0.007, 0.007, 0.006, 0.006,
0.006, 0.006, 0.006, 0.006, 0.005, 0.005, 0.005, 0.005, 0.004,
0.004, 0.004, 0.004, 0.004, 0.003, 0.003, 0.003, 0.003, 0.003,
0.002, 0.002, 0.002, 0.002, 0.002, 0.002, 0.001, 0.001, 0.001,
0.001, 0.001, 0.001, 0.001, 0.001, 0.001, 0.001, 0.001, 0.000,
0.000]

# Error bar data here
Xcorr_points_err = 0.0001*ones(len(Xcorr_points))
Powercorr_points_err = 0.01*ones(len(Powercorr_points))

# Define the residuals to be minimized
#
def residuals(w0, y, x):
err = y - 0.5*(1.0+erf(x/w0))
return err
# Define the fit function: 0.5*(1.0 + erf(x/w0))
#
def peval(x, w0):
return 0.5*(1.0 + erf(x/w0))
# Generate the arrays needed to make a smooth plot of the
guess function
Xcorr_inch_fit =
linspace(min(Xcorr_points),max(Xcorr_points),106)
Powercorr_guess = peval(Xcorr_inch_fit, w0)

# Run the least squares function to minimize the residuals
plsq = leastsq(residuals, w0, args=(Powercorr_points,
Xcorr_points))
print(plsq[0])

```

---

```

# Generate the arrays needed to make a smooth plot of the fit
function
Powercorr_fit = peval(Xcorr_inch_fit, plsq[0])

# Define the limits of the horizontal axis
xlim(min(Xcorr_points),max(Xcorr_points))

# Label the horizontal axis, with units
xlabel("$x_{1/2}$-x$ [inch]", size = 16)

# Define the limits of the vertical axis
ylim(min(Powercorr_points),max(Powercorr_points))

# Label the vertical axis, with units
ylabel("(P-P_{bkgd})/P_{max}$", size = 16)

# Make a grid on the plot
grid(True)

# Generate the plot. The plot symbols will be green (g)
circles (o).
#plot(Xcorr_points,Powercorr_points,"go",label="Data")
errorbar(Xcorr_points,Powercorr_points,xerr=Xcorr_points_err,y
err=Powercorr_points_err,fmt="go",label="Data")
plot(Xcorr_inch_fit,Powercorr_guess,"r--",label="Guess")
plot(Xcorr_inch_fit,Powercorr_fit,"b",label="Fit")
legend(loc=2)
show()

```

e. PYTHON CODE FOR PLOTTING THE RAW POWER AND STAGE READINGS FOR  
THE BEAM PROFILE—SINGLE-MODE OPTICAL FIBER

```

#
# PHY692_Plot_Of_Power_And_Stage_Raw_Readings
# Using_Optical_Fiber_For_Laser_TEM00_Mode.py
#
# This file will generate a plot of
# the raw power reading versus the raw stage reading
# using optical fiber for laser TEM00 mode
#
# Written by:
#
# Ernest R. Behringer
# Department of Physics and Astronomy
# Eastern Michigan University

```

---

```

# Ypsilanti, MI 48197
# (734) 487-8799
# ebehringe@emich.edu
#
# 20150127 by ERB
#
# Modified by:
# Najwa Sulaiman
# Department of Physics and Astronomy
# Eastern Michigan University
# Ypsilanti, MI 48197
# nsulaima@emich.edu
#
# 20150624 by NS
# 20150716 by NS
# 20150720 by NS
# 20150823 by NS
# 20160313 by NS
#

import pylab as p
import numpy as np

X_Points = np.linspace(0.5250, 0.6100, 86)
P_Points = [0.000, 0.000, 0.000, 0.000, 0.000, 0.000, 0.000,
0.000, 0.000, 0.000, 0.000, 0.000, 0.000, 0.000, 0.000, 0.000,
0.000, 0.000, 0.000, 0.000, 0.001, 0.001, 0.001, 0.002, 0.002,
0.002, 0.003, 0.005, 0.011, 0.021, 0.037, 0.053, 0.070, 0.098,
0.146, 0.210, 0.279, 0.348, 0.412, 0.496, 0.588, 0.692, 0.807,
0.963, 1.087, 1.240, 1.385, 1.507, 1.557, 1.533, 1.469, 1.389,
1.307, 1.196, 1.065, 0.916, 0.710, 0.596, 0.457, 0.380, 0.323,
0.263, 0.205, 0.144, 0.102, 0.077, 0.055, 0.034, 0.028, 0.020,
0.009, 0.009, 0.008, 0.006, 0.005, 0.004, 0.003, 0.003, 0.002,
0.002, 0.002, 0.002, 0.001, 0.001, 0.000, 0.000]

# Error bar data here
X_points_err = 0.001*p.ones(len(X_Points))
Powercorr_points_err = 0.01*p.ones(len(P_Points))

p.xlim(min(X_Points),max(X_Points))
p.ylim(min(P_Points),max(P_Points))

p.xlabel("Raw stage reading $x$ [inches]", size = 16)
p.ylabel("Transmitted power $P$ [nW]", size = 16)
p.grid(True)

```

---

```
p.errorbar(X_Points,P_Points,xerr=X_points_err,yerr=Powercorr_
points_err,fmt="go")
p.plot(X_Points,P_Points,"b")
p.show()
```

f. PYTHON CODE FOR EVALUATING THE LASER BEAM DIAMETER FOR BEAM  
PROFILE—SINGLE-MODE OPTICAL FIBER

```
#
# PHY697_Fiber-sampled_TEM00_v5.py
#
# This file will calculate the double integral
# of the TEMmn mode over a circular area
# that represents the input aperture of a fiber optic
# that is scanned along the x-direction
#
# Written by:
#
# Ernest R. Behringer
# Department of Physics and Astronomy
# Eastern Michigan University
# Ypsilanti, MI 48197
# (734) 487-8799
# ebehringe@emich.edu
#
# 20150701 by ERB, using earlier code from NS and ERB
# 20150708 by ERB, correcting modification by NS
# 20160517 by NS

# import the commands to generate/manipulate values, and do
integration
from numpy import linspace,sqrt,exp,zeros,ones
from scipy.integrate import nquad
from scipy.special import eval_hermite

# import the commands needed to make the plot
from pylab import
plot,xlim,xlabel,ylim,ylabel,grid,show,title,legend
from matplotlib.pyplot import errorbar

# input variables
I0 = 1.0 # maximum irradiance [mW/um2]
m=0 # order of the Hermite polynomial in the x direction
n=0 # order of the Hermite polynomial in the y direction
R = 62.5 # radius of the fiber [um]
```

---

```

w = 250.0 # beam radius [um]
mpts = 2 # number of vertical positions for the detector
aperture
yc = linspace(-0.0001,0.0001,mpts+1) # vertical position of
the center of the fiber optic [um]
npts = 67 # number of points at which the power is measured
# horizontal position of the center of the fiber optic
xc = linspace(-640.0,760.0,npts+1)
# Powercorr_points contains the dependent variable values
(measurements).
# Optical power readings (no-units)
Powercorr = [0.000, 0.000, 0.001, 0.001, 0.001, 0.001, 0.001,
0.001, 0.002, 0.003, 0.007, 0.013, 0.024, 0.034, 0.045, 0.063,
0.094, 0.135, 0.179, 0.224, 0.265, 0.319, 0.378, 0.444, 0.518,
0.618, 0.698, 0.796, 0.890, 0.968, 1.000, 0.985, 0.943, 0.892,
0.839, 0.768, 0.684, 0.588, 0.456, 0.383, 0.294, 0.244, 0.207,
0.169, 0.132, 0.092, 0.066, 0.049, 0.035, 0.022, 0.018, 0.013,
0.006, 0.006, 0.005, 0.004, 0.003, 0.003, 0.002, 0.002, 0.001,
0.001, 0.001, 0.001, 0.001, 0.001, 0.000, 0.000]

# Error bar data here
xc_err = 0.0001*ones(len(xc))
Powercorr_err = 0.01*ones(len(Powercorr))

# scaled variable values
# Note that all lengths are 'scaled' by R (fiber radius).
w_sc = w/R
yc_sc = yc/R
xc_sc = xc/R
xcsc = 0.0 # an initial value just as a placeholder
ycsc = 0.0 # an initial value just as a placeholder

# define array of powers, with initial values of zero
power = zeros((mpts+1,npts+1))

# define the function that we are integrating - note that x
and y are scaled
def f(x,y):
return I0 * ((eval_hermite(m, sqrt(2)*x/w_sc)*exp(-
x**2/w_sc**2))**2) * (eval_hermite(n, sqrt(2)*y/w_sc)*exp(-
y**2/w_sc**2))**2

def bounds_x():
return [xcsc-1,xcsc+1]

# define the bounds of y

```

---

```

def bounds_y(x):
return [ycsc - sqrt(1.0-(x-xcsc)**2),ycsc + sqrt(1.0-(x-
xcsc)**2)]

# loop over vertical positions
for j in range(0,mpts+1):
ycsc = yc_sc[j]
# loop over horizontal positions
for i in range(0,npts+1):
# update xcsc
xcsc = xc_sc[i]
# perform the integration using nquad
# NOTE that the order in which the bounds are given in the
# nquad argument is [inner integration bounds, outer
integration bounds]
# NOTE also that the output of nquad consists of two elements:
# the first element is the value of the integral
temp = nquad(f, [bounds_y, bounds_x])
power[j][i] = temp[0]
# Define the limits of the horizontal axis
xlim(min(xc),max(xc))

# Label the horizontal axis, with units
xlabel("Fiber optic position $x$ [$\mu m$]", size = 16)

# Define the limits of the vertical axis
ylim(0.0,1.0)

# Label the vertical axis, with units
ylabel("Scaled power $P$ ", size = 16)

# Make a grid on the plot
grid(True)

# Make the plot title
title("Fiber radius $R$ = %s $\mu m$, beam radius $w$ = %s
$\mu m$"%(R,w))

# Generate the plot.
errorbar(xc,Powercorr,xerr=xc_err,yerr=Powercorr_err,fmt="go",
label="Data")
plot(xc,power[0]/max(power[0]),"b-",label="Theory")
legend(loc=2)

# Show the plot
show()

```

---

g. PYTHON CODE FOR PLOTTING THE SENSITIVITY OF THE COUPLING OF THE  
FREE SPACE BEAM TO THE FIBER

```
#
# PHY692_Plot_Of_Power_And_Stage_Fiber_Efficiency.py
#
# This file will generate a plot of
# the power reading versus the stage reading
# for measuring the fiber efficiency.
#
# Written by:
#
# Ernest R. Behringer
# Department of Physics and Astronomy
# Eastern Michigan University
# Ypsilanti, MI 48197
# (734) 487-8799
# ebehringe@emich.edu
#
# 20150127 by ERB
#
# Modified by:
# Najwa Sulaiman
# Department of Physics and Astronomy
# Eastern Michigan University
# Ypsilanti, MI 48197
# nsulaima@emich.edu
#
# 20150624 by NS
# 20150716 by NS
# 20150823 by NS
# 20160402 by NS
#
import pylab as p
import numpy as np

X_Points = np.linspace(0.1580, 0.2210, 127)
P_Points = [199.7, 200.1, 200.6, 201.0, 201.6, 201.9, 202.2,
202.8, 203.2, 203.4, 204.0, 204.3, 204.6, 205.2, 205.5, 206.1,
206.5, 206.9, 207.2, 207.5, 207.9, 208.3, 208.6, 209.1, 209.4,
209.7, 210.0, 210.3, 210.7, 211.0, 211.1, 211.5, 211.8, 212.0,
212.3, 212.6, 212.7, 212.9, 213.2, 213.5, 213.7, 214.1, 214.2,
214.4, 214.4, 214.5, 214.6, 214.7, 215.0, 215.2, 215.5, 215.5,
215.5, 215.6, 215.7, 215.8, 216.2, 216.3, 216.3, 216.5, 216.6,
216.8, 217.0, 217.2, 217.5, 217.7, 217.8, 218.1, 218.2, 218.3,
```



---

```
218.4, 218.4, 218.4, 218.4, 218.4, 218.5, 218.4, 218.4, 218.4,
218.3, 218.3, 218.3, 218.2, 218.1, 218.0, 217.9, 217.8, 217.6,
217.6, 217.5, 217.2, 216.9, 216.6, 216.3, 216.1, 215.8, 215.4,
214.9, 214.6, 214.2, 214.0, 213.5, 213.1, 212.8, 212.3, 211.7,
211.0, 210.5, 209.9, 209.2, 208.5, 208.0, 207.4, 206.7, 206.0,
205.5, 204.7, 203.9, 203.4, 203.0, 202.4, 201.6, 201.0, 200.9,
200.2, 200.0, 199.7]
```

```
# Error bar data here
X_points_err = 0.0005*p.ones(len(X_Points))
Powercorr_points_err = 0.01*p.ones(len(P_Points))

p.xlim(min(X_Points),max(X_Points))
p.ylim(min(P_Points),max(P_Points))

p.xlabel("Optical Fiber position $z$ [inches]", size = 16)
p.ylabel("Transmitted power $P$ [$\mu$W]", size = 16)
p.grid(True)
p.errorbar(X_Points,P_Points,xerr=X_points_err,yerr=Powercorr_
points_err,fmt="go")
p.plot(X_Points,P_Points,"b")
p.show()
```

---

## APPENDIX B: CALCULATIONS FOR BEAM PROFILE

### a. CALCULATING THE DIAMETER OF A BEAM

For calculating the beam diameter, we first determine  $x_{1/2}$  where  $x_{1/2}$  is the position where  $\frac{P(x)-P_{bkgd}}{P_{max}} = 0.5$ , where  $P_{max} = P_{peak} - P_{bkgd}$ .<sup>9</sup> To find  $x_{1/2}$  we need to divide the transmitted power data by the maximum obtained power. Then we look where the two closest data to 0.5 are. After defining the two data, we see what stage readings correspond to these data.

Let

$$P'_{1,2} \equiv P_{1,2}/P_{max} \quad \text{where } P_{1,2} \text{ are the two closest power readings to } P=0.5$$

where

$$P_1 < 0.5 < P_2$$

Then,

$$\frac{P'_2 - P'_1}{x_2 - x_1} = \text{slope}$$

Where  $x_{1,2}$  are the corresponding stage readings.

Then,

$$\frac{0.5 - P'_1}{x_{1/2} - x_1} = \text{slope}$$

Then,

$$x_{1/2} = \frac{0.5 - P'_1}{\text{slope}} + x_1$$

After finding  $x_{1/2}$ , we subtract the stage readings from  $x_{1/2}$  and plot it in python program or evaluating the diameter. The Python code will give us the best value for ( $w_o$ ), then we use the relation:

---


$$\frac{P(x)-P_{bkgd}}{P_{max}} = \frac{1}{2} + \frac{1}{2} \operatorname{erf}\left(\frac{x}{w_0}\right)$$

Which can be derived by assuming a Gaussian beam profile for the TEM<sub>00</sub> mode:

$$I(x_{\pm}) = I_{max} e^{-2x^2/w_0^2}$$

When  $I(x_{\pm}) = \frac{1}{2} I_{max}$  Then the radius of the laser beam is:

$$x_{\pm} = w_0 \sqrt{\frac{\ln 2}{2}}. \text{ Consequently, } 2x_{\pm} = w_0 \sqrt{2(\ln(2))} \text{ which is the beam diameter.}$$

b. CALCULATING  $I_{0mn}$

Having the relation:

$$I_{mn}(x, y) = I_{0m} \exp\left[\frac{-2(x^2 + y^2)}{w_0^2}\right] H_m^2\left(\frac{x\sqrt{2}}{w_0}\right) H_n^2\left(\frac{y\sqrt{2}}{w_0}\right)$$

$$\text{Let } u = \left(\frac{x\sqrt{2}}{w_0}\right) \rightarrow u^2 = \frac{2x^2}{w_0^2} \rightarrow du = \frac{\sqrt{2}}{w_0} dx$$

$$v = \left(\frac{y\sqrt{2}}{w_0}\right) \rightarrow v^2 = \frac{2y^2}{w_0^2} \rightarrow dv = \frac{\sqrt{2}}{w_0} dy$$

Then,

$$I_{mn}(x, y) = I_{0mn} \left(\frac{w_0^2}{2}\right) \exp[-(u^2 + v^2)] H_m^2(u) H_n^2(v)$$

$$P_{max} = I_{0mn} \left(\frac{w_0^2}{2}\right) \int_{-\infty}^{\infty} du \int_{-\infty}^{\infty} dv \exp(-u^2) \exp(-v^2) H_m^2(u) H_n^2(v)$$

But,

$$\int_{-\infty}^{\infty} H_m(x) H_n(x) \exp(-x^2) dx = \sqrt{\pi} 2^n n! \delta_{nm}$$

Then,

$$I_{0mn} = \frac{2 P_{max}}{w_0^2 \pi (2^m n!) (2^n n!)}$$